The final publication is available at

http://dx.doi.org/10.1039/c3dt53181c

Additional Information

Layered zeolitic materials: An approach to design versatile functional solids.

Urbano Díaz, Avelino Corma*

Instituto de Tecnología Química, UPV-CSIC, Universidad Politécnica de Valencia,
Avenida de los Naranjos s/n, E-46022 Valencia, Spain
*e-mail (corresponding author): acorma@itq.upv.es; Web: http://www.itq.upv-csic.es/; Fax: +34 963 877 809; Tel: +34 963 877 800

Abstract

Relevant layered zeolites have been considered in this perspective article from the point of view of the synthesis methodologies, materials characterization and catalytic implications, considering the unique physico-chemical characteristics of lamellar materials. The potentiality of layered zeolitic precursors to generate novel lamellar accessible zeolites through swelling, intercalation, pillarization, delamination and/or exfoliation treatments is studied, showing the chemical, functional and structural versatility exhibited by layered zeolites. Recent approaches based on assembly of zeolitic nanosheets which act as inorganic structural units through the use of dual structural directing agents, the selective modification of germanosilicates and the direct generation of lamellar hybrid organic-inorganic aluminosilicates are also considered to obtain layered solids with well-defined functionalities. The catalytic applications of the layered zeolites are also highlighted, pointing out the high accessibility and reactivity of active sites present in the lamellar framework.

1- Introduction

The study of natural clays showed the ability of layered inorganic materials to generate a large number of derived solids by intercalation of different organic or inorganic guests in the interlayer space.[1] Furthermore, chemical processes, such as solvation of interlayered cations which facilitates the separation between the layers,[2] and even mechanical-physical processes, such as ultrasonic methods, stirring, freeze-drying or centrifugation systems, have allowed to obtain novel layered solids from starting lamellar precursors. The materials obtained exhibit extremely interesting physico-chemical properties that can find applications in different industrial fields.[3]

In general, layered inorganic materials are structurally conformed by a consecutive repetition of individual sheets located in parallel spatial planes, being electrostatically bonded by weak Van der Waals interactions or hydrogen bonds, along the perpendicular plane in which the layers are disposed. This structural conformation is present in a great number of inorganic materials, from clays or silicates to other structurally more complex such as layered double hydroxides,[4] metallic layered materials or carbonaceous solids (graphenes[5] or graphites).[6] Among them, layered zeolitic materials and their derived solids are particularly attractive because combine high thermal and mechanical stability with high reactivity, without losing the intrinsic versatility exhibited by the layered solids.

We will show here, the main layered zeolitic materials reported up to now together with preparation methods and applications, which are mostly focused on the design of catalysts with well-defined single isolated and accessible sites. Advantages and disadvantages will also be highlighted, showing associated alternative synthesis routes and modifications to prepare novel versatile functional lamellar catalysts.

2- Layered zeolitic materials derived from bi-dimensional (2D) precursors

Within the zeolite family, it is possible to find different examples in which their final tri-dimensional (3D) structure is achieved through stable intermediate layered zeolitic precursors obtained during hydrothermal synthesis processes. In those cases, after removing the structural directing agents (SDAs) located in the interlayer space by calcination treatments, contiguous layers are connected generating the corresponding 3D zeolite. However, the presence of individual layers separated between them by ionic species, which are compensating the charges of zeolitic sheets in these 2D zeolite precursors, facilitates, as it occurs with clays, swelling, pillarization, intercalation or exfoliation/delamination processes, being possible to obtain novel layered materials with higher pore sizes. Thus, in turn to improve the accessibility of different molecules to framework active sites, without losing the physico-chemical properties characteristic of conventional microporous zeolites.[7]

2.1- Bi-dimensional (2D) layered zeolitic precursors

It has been reported an increasing number of thermally stable layered zeolite precursors, *i.e.*, stable layered aluminosilicates that either by calcination or by hydrothermal transformation can yield 3D zeolites. Among them, we could highlight three main groups of lamellar precursors related with the topologies MWW, FER and NSI, considering the IZA

nomenclature, being the two last also structurally related with the CDO and CAS frameworks, respectively.[8, 9] Through these stable precursors, it should be possible to obtain other pillared and delaminated (exfoliated) materials by post-synthesis treatments (Figure 1 and Table 1).
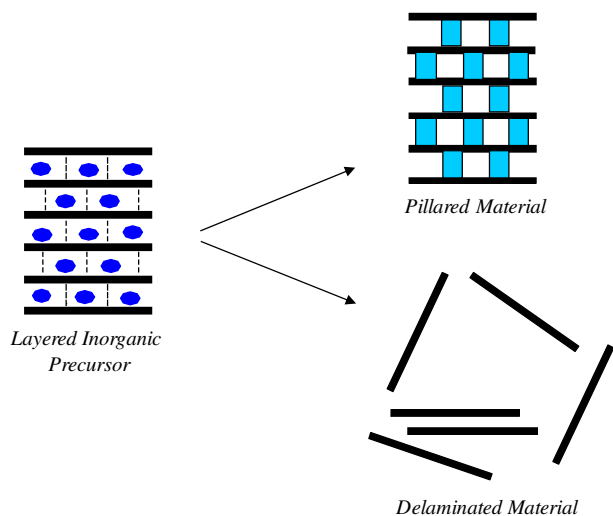

Layered Inorganic Precursor

Pillared Material

Delaminated Material

Figure 1. Layered materials derived from inorganic precursors.

Table 1. Most relevant layered zeolitic materials.

Family (IZA code)	2D Layered Precursor	3D Zeolite	Pillared or Expanded	Delaminated or Exfoliated	Other
MWW	MWW(P) (MCM-22(P))	MCM-22 MCM-49 PSH-3 SSZ-25 ITQ-1 ERB-1 Ti-MWW	MCM-36 MWW-BTEB IEZ-MWW Ti-YNU-1	ITQ-2 UCB-1 Del-Ti-MWW	MCM-56 ITQ-30 EMM-10 (partial exfoliation)
FER	PREFER PLS-3	Ferrierite	ITQ-36 IEZ-FER	ITQ-6 ITQ-20	MCM-47 ERS-12 ITQ-19 (stacking FER layers)
CDO	MCM-65 USZ-25 PLS-1 PLS-4 HUS-4	CDS-1	IEZ-CDO		
NSI	Nu-6(1)	Nu-6(2)	MCM-39	ITQ-18	
CAS	EU-19 MCM-69	EU-20			EU-20-Polymorphs
MFI	Multilamellar-MFI	ZSM-5 TS-1	Pillared-Multilamellar-MFI	Unilamellar-MFI SPZ	

PCR (UTL Ge-Zeolites)	ICP-1P Dislodged-IM-12	ICP-1 ICP-4 COK-14	ICP-1PI ICP-2 (IEZ-type)

The first known 2D layered zeolitic precursor exhibits MWW topology, being formed by parallel and ordered zeolitic layers perpendicular to the *c* axis. Each individual MWW-type layer has a thickness of 2.5 nm and contains a 10 member-ring (MR) sinusoidal channel present along the plane *ab* (Figure 2). Onto the external surface of each zeolitic sheet, there is a large amount of terminal silanol groups (Si-OH) which condense, after the calcination process, with other silanols present in contiguous layers generating the 3D zeolitic structure. Due the collapse of the layers, formation of an additional second pore system conformed by hemi-cavities delimited by 12 MR from the semi-cups located in the surface of each MWW layer is favored. In Figure 2, it is observed the detailed structure of the layered zeolitic precursor MWW(P).[10]
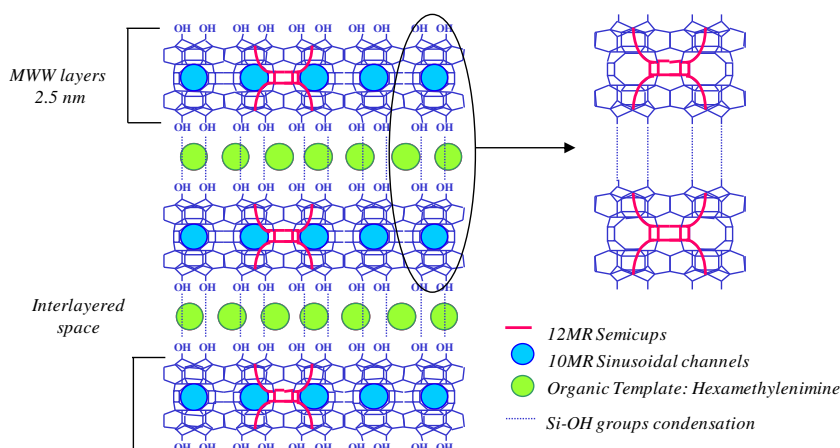

Figure 2. Artistic representation of MWW(P) layered zeolitic precursor.

The 3D MWW zeolitic material obtained after the elimination of the organic template was patented as MCM-22 by Rubin *et al.*, in 1990.[11] However, this structure was identical to another aluminosilicate PSH-3 synthesized by Puppe *et al.* in 1984.[12] Both zeolites were prepared using hexamethylenimine (HMI) as Structure Directing Agent (SDA). Studies carried out by Leonowicz *et al.* confirmed that the structure of MCM-22 is formed by two independent porous systems, being both accessible through 10 MR windows. One of these systems is defined by sinusoidal and bidirectional channels with 0.52 nm of internal diameter. The second porous system is formed by super-cavities with a free internal diameter close to 0.71 nm delimited by 12 MR, exhibiting an internal height of 1.82 nm. The super-cavities are connected between them through 10MR windows. In Figure 3, the schematic structure of MCM-22 with the two independent porous systems is shown. It has to be pointed out that that the 3D MWW zeolite type can also be directly synthesized without passing through the intermediate layered precursors, and the resultant product was named by Exxon Mobil as MCM-49 zeolite.[13] In this case, the direct crystallization of collapsed MWW materials was achieved by optimizing the HMI/Na$^+$ molar ratio and the aging step of the synthesis gel.[14]
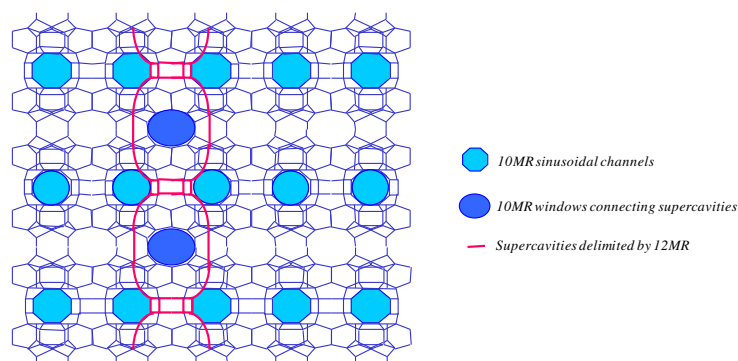
Figure 3. Artistic representation of zeolite MCM-22.

The layered zeolitic precursor MWW(P) can be obtained with high crystallinity in Si/Al molar ratios between 15 and 70. However, when the aluminum content decreases in the synthesis gel (Si/Al > 70), MFI-type phases are detected as impurities. Normally, the synthesis is performed in alkaline medium, using sodium as charge compensating cation and under rotating or stirring conditions. [15, 16] However, if the synthesis is carried out in static, the crystallization of MWW(P) is more difficult and other phases such as Ferrierite or Mordenite coexist.[17] Nevertheless, previous aging of the synthesis gel at temperatures higher than 180ºC favors the formation of highly crystalline MWW(P) precursor.[18]

In 1987, Zones *et al.* patented an aluminosilicate named as SSZ-25 which exhibited characteristics similar to MWW materials.[19] Initially, it was supposed that this material was formed by only one type of porous channel delimited by 12 MR,[20] but it was confirmed that the SSZ-25 is isomorphic to PSH-3, being also obtained through the collapse of the previous synthesized layered zeolitic precursor. [21] In this case, during the preparation of the SSZ-25 precursor, potassium and trimethyladamantamonium hydroxide (TMAda$^+$OH$^-$) were used instead of sodium and HMI, respectively.[22]

MWW(P) was always obtained in the presence of trivalent cations,[23] until the synthesis of a pure silica precursor of MWW that, after collapse, generates a pure silica 3D MWW crystalline phase that was named ITQ-1.[24] The layered precursor of ITQ-1 was synthesized with two organic templates such as TMAda$^+$OH$^-$ and HMI in alkaline medium. It was observed that the HMI molecules stabilize the 10 MR sinusoidal channels present in the internal structure of MWW layers, and the TMAda$^+$ cationic species allow the formation of external semi-cups delimited by 12 MR located in the surface of the zeolitic sheets. Different attempts were performed to introduce tetrahedral titanium into the structure of the purely siliceous ITQ-1 precursors directly in the synthesis route. However, the alkaline conditions present in the gel prevented the effective incorporation of titanium into the zeolitic network due the fast precipitation of amorphous titanium-silicates in the synthesis medium.[25, 26]

In 1988, Bellussi *et al.* prepared the microporous borosilicate named ERB-1 that is also isostructural with the aluminosilicate MCM-22, and which was also obtained through a layered zeolitic precursor formed by ordered MWW layers.[27] In this case, piperidine was used as template instead of HMI or TMAda$^+$ employed in the synthesis of MCM-22, SSZ-25 or ITQ-1 precursors. Aluminium was also incorporated into the lamellar network of ERB-1 materials together with the tetrahedrally coordinated boron, although a high content of aluminum implied a marked decrease in the boron incorporation.[28]

The influence of the sodium cations in the crystallization of ERB-1 layered precursor is not significant because in the final product it was not detected as compensating cation. This observation opened the door to prepare layered zeolitic precursors with MWW topology in absence of alkaline metals, allowing then the use of titanium alkoxides for the direct incorporation of tetrahedral titanium into the framework of this type of 2D materials. It is known that the presence of alkaline cations in the synthesis slurry facilitates the amorphous silicotitanates precipitation which avoids the integration of titanium coordinated into the network of zeolitic layers,[29] being this factor not relevant in the preparation of ERB-1 layered precursors where alkaline cations are not necessary. Then Tatsumi *et al.* have prepared MWW crystalline precursors with tetrahedrally coordinated boron and titanium in the final structure, and, from this precursor, a B-free titanosilicate with the MWW topology (Ti-MWW) was prepared.[30]   Specifically, the synthesis first involved the preparation of ERB-1 and the consecutive deboronation through calcinations and acid extraction treatments by consecutive cycles, to obtain a highly siliceous solid. The layered MWW silicate obtained was treated with titanium alkoxide sources in an aqueous solution of cyclic amines such as piperidine, hexamethylenimine, pyridine, piperazine, etc. The material finally synthesized is a B-free zeolite with a conventional MWW lamellar organization, containing tetrahedrally coordinated titanium in the individual zeolitic layers (Figure 4). This synthesis methodology to obtain Ti-MWW precursors through reversible structural conversions was certainly innovative.[31, 32]
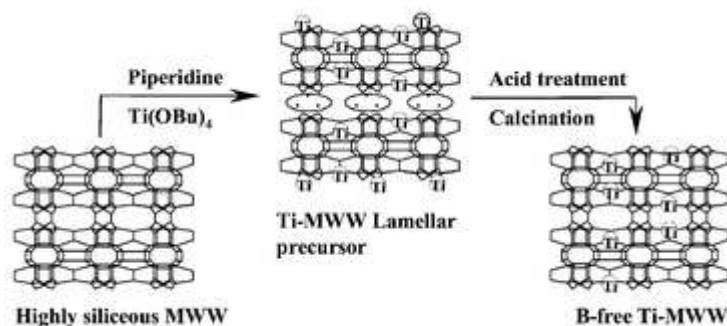

Figure 4. Synthesis route to obtain B-free Ti-MWW layered precursors (according to ref. 31).

Also, it is important to point out that different MWW(P) layered precursors were prepared containing other tetrahedrally coordinated metals within the individual MWW layers, such as gallium,[33] vanadium,[34] lanthanum or cerium.[35] The incorporation of these metallic species was achieved by hydrolysis and condensation of silicon reagents with metallic salts in moderate acidic media followed by a switch of synthesis media to basic conditions during the hydrothermal process.

Another relevant family of layered zeolitic precursors formed by ordered FER-type sheets is reported in the state-of-art, being the structural characteristics of these layers similar to CDO framework topology (CDS-1 zeolite[36]) exhibited by different layered silicates such as MCM-65, USZ-25, PLS-1, PLS-4 and HUS-4 (Table 1).[37, 38, 39, 40] Within this group of layered materials, the lamellar precursor named PREFER synthesized by Schereyeck *et al.* in 1995 is the most significant.[41] This bi-dimensional material is formed by ordered ferrieritic layers perpendicularly disposed to axis *a*, separated between them by 4-amino-2,2,6,6-tetrametilpiperidina molecules which act as structural directing agents. The synthesis was

normally carried out in fluoride medium.[42, 43] The absence of alkaline cations in the synthesis media allowed the introduction of tetrahedral titanium in the ferrieritic layers framework of PREFER.[44] In Figure 5, it is shown the 2D PREFER structure and the 3D Ferrierite obtained after the covalent linkage between the zeolitic layers during the condensation phenomenon favored by the calcination treatment.
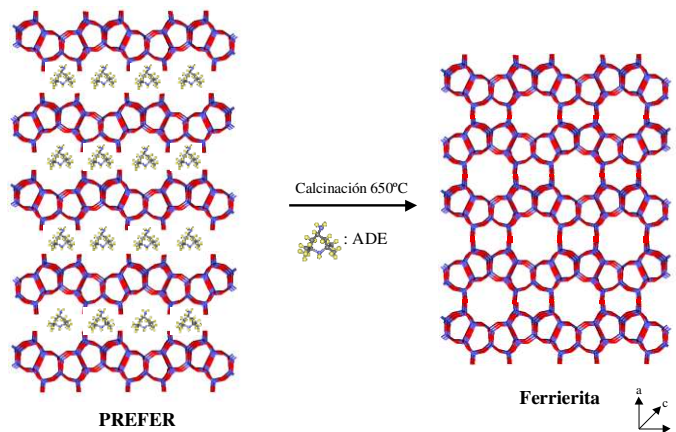

Calcinación 650ºC

: ADE

PREFER

Ferrierita

Figure 5. Artistic representation of the condensation effect from layered precursor PREFER to obtain Ferrierite zeolites.

The scheme in Figure 5 is useful to understand that the structure of the PREFER precursor is formed by individual ferrieritic layers with ~0.9 nm thickness, structured by assembled 5 MR units linked between them through two shared oxygen atoms. After the calcination process, the zeolitic layers are covalently connected, and the 2D PREFER is transformed into the 3D Ferrierite zeolite formed by linked pentasils which are organized in $[5^4]$ polyhedral units (Figure 5). The final Ferrierite exhibits an orthorrombic symmetry conformed by two intercrossed channels, respectively delimited by 10 MR (0.42x0.54 nm) along axis *c* and by 8 MR (0.35x0.42 nm) along axis *b*. Wider void spaces, with internal diameters around 0.6-0.7 nm, are generated in the crossing of the microporous channels. It is important to point out that the PREFER is only synthesized in presence of 4-amino-2,2,6,6-tetramethylpiperidine, acting as structural directing agent (ADE). When other heterocyclic amino molecules are used as template, the 3D Ferrierite is directly obtained and the layered intermediate precursor is not detected. The PREFER has also been obtained from layered silicate H-kanemite as silica source and tetramethylammonium hydroxide as structure directing agent, being called in this case PLS-3.[45, 46]

Within the PREFER zeolitic precursors, Lobo *et al.* synthesized the MCM-47 zeolite from its corresponding layered material,[47] following previous studies reported by Szostak *et al*. and Valyocsik *et al*.[48, 49] Specifically, di-quaternary ammonium salts prepared from 1-methylpyrrolidine and 1,4-dibromebutane were used as specific structural directing agents. The lamellar precursor of MCM-47 is analogous to PREFER except for a slight displacement, along the *b* axis and half unit cell displacement in the spatial situation of ferrieritic layers is detected from structural resolution studies (Figure 6). This phenomenon would explain the differences observed in the X-ray patterns between both layered precursors. Obviously, after calcination, the 3D MCM-47 is formed by individual FER layers which are not completely connected because the silanols of consecutive sheets are not hydrolyzed and condensed. Similarly, a layered silicate named ERS-12, also composed by a regular stacking of ferrierite

layers with tetramethylammonium (TMA) cations located in the interlayer region was obtained, exhibiting similar structuration to MCM-47 lamellar precursor.[50]
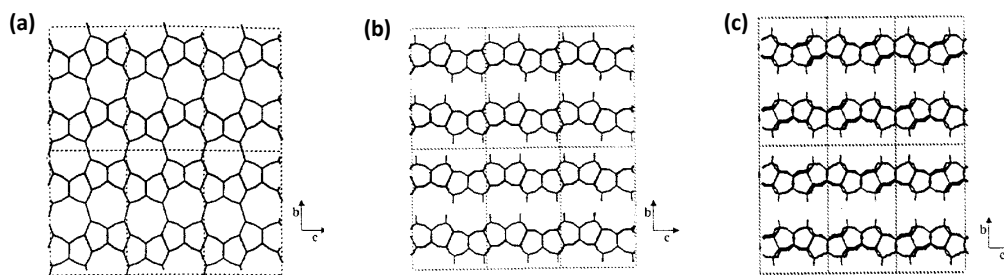

Figure 6. Structural representation of FER materials: (a) Ferrierite, (b) MCM-47 and (c) PREFER (from reference 47).

Recently, another layered zeolitic material, so-called ITQ-19, was obtained being isomorphically identical to precursor of MCM-47. But, it was prepared with high amounts of tetrahedral aluminum finally incorporated in the ferrieritic layers structure. The ITQ-19 was synthesized using 1,4-diazabicycle[2,2,2]octane as template and the corresponding 3D ferrieritic zeolite was obtained after acalcination process.[51] It is remarkably that the use of two combined structural directing agents such as quinuclidine and 1-benzyl-1-methylpyrrolidinium favored the preparation of layered zeolitic materials containing ferrierite layers. In this last case, computational results suggested that quinuclidine molecules were too bulky to be accommodated inside the cages of full-sheet connected 3D FER and lamellar materials with a higher interlayer separation were finally obtained (Figure 7).[52]
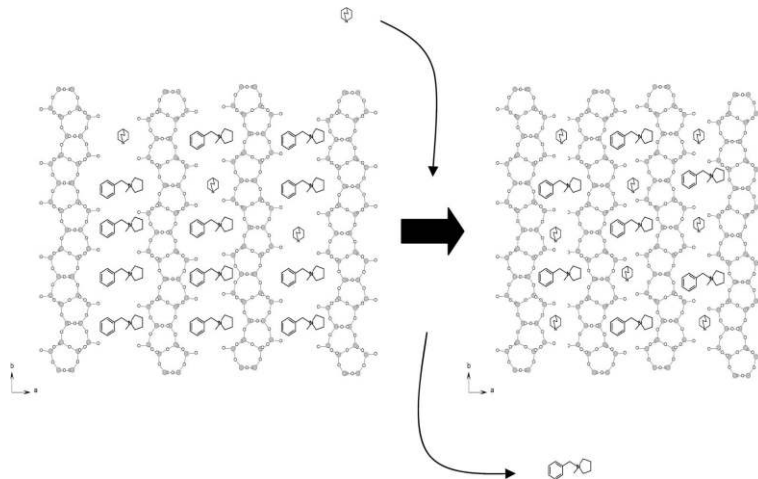

Figure 7. Mechanism of crystallization of the layered Ferrierite-like materials, using quinuclidine and 1-benzyl-methylpyrrolidinium as structural directing agents (from reference 52).

The third group of layered zeolitic precursors is formed by aluminosilica sheets with NSI topology also structured by 5 MR units like the above commented PREFER, but spatially disposed with different symmetry. Inside this family, the Nu-6(1) is the most relevant zeolitic precursor synthesized from hydrothermal conditions in presence of 4,4'-bipyridil molecules as template which are localized in two crystallographically different positions (Figure 8a).[53,] The structure of the Nu-6(1) precursor is similar to those previously described for layered silicates so-called EU-19 and MCM-69 (Table 1),[54, 55] although the interlayer space in these last precursors is lower due to the shorter size of the hosted molecules, favoring modifications in

the stacking parameter. This fact induced different symmetries in the different NSI and CAS layered precursors.

After thermal treatment for SDA removing in the Nu-6(1), the small-pore pentasil Nu-6(2) zeolite is obtained by layers condensation, being this 3D microporous zeolite characterized by a one-dimensional channel system of two independent and non-equivalent sets of 8 MRs which alternate along the crystallographic axis *c* (named as A and B in Figure 8b).[56, 57] It is notorious the close structural relation between Nu-6(2) and the orthorhombic cesium aluminosilicate EU-20 (IZA code CAS), being both built by applying different symmetries to the same pentasil periodic building unit (Figure 8c).[58, 59, 60] Although the structure of EU-20 is currently unknown, the isomorphical structure observed between Nu-6(1) and EU-19, would suggest that the structure of the EU-20 is similar to Nu-6(2). It is remarkable that different EU-20 polymorphs with several stacking organization of the NSI-type layers were also observed after hydrothermal treatments.[61]
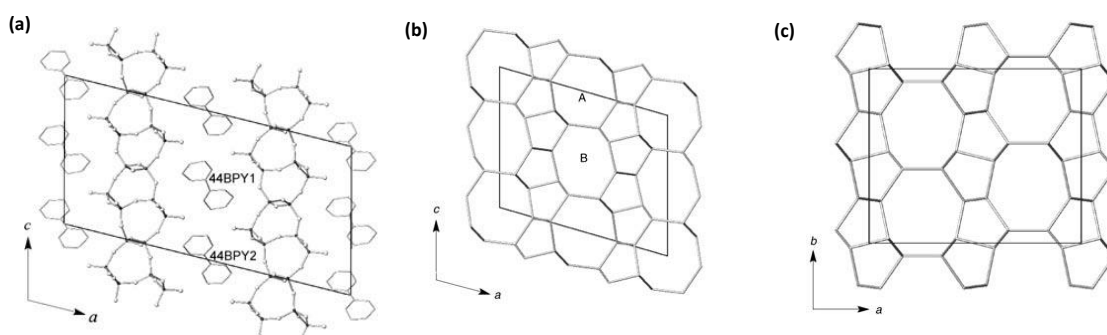

Figure 8. Structural representation of (a) Nu-6(1), (b) Nu-6(2) and EU-20 (following reference 57).

2.2- Pillared and expanded zeolites

The bi-dimensional layered zeolitic precursors, studied in the previous section, exhibit the ability to modify their structural characteristics through consecutive steps, taking advantage of the free space present between contiguous ordered inorganic layers. In this way, it is possible to obtain novel, more accessible porous materials due to the intercalation in the interlayered space of organic or inorganic compounds which act as pillars. This phenomenon avoids the covalent connection between the consecutive inorganic layers, after the removing of the ionic molecules which are compensating the surface charges present in the sheets, generating additional mesoporous galleries located in the interlayer space. Furthermore, this intercalation process would allow not only to increase the accessibility to internal space of microporous zeolites, but also to incorporate additional active sites located between the inorganic zeolitic sheets. These layered solids are, generally, named as *pillared zeolitic materials*.[62, 63]

Within the MWW family, Kresge *et al.* reported the MCM-36 zeolite as the first pillared zeolite which is formed by MWW-type inorganic layers.[64] The preparation of this material was based on an initial swelling step achieved by cationic exchange of alkylammonium molecules (preferably $C_{16}TMA^+OH^-$) which were placed in the interlayer space separating the MWW layers between them along to axis *c*. In a second step, the swollen precursor was pillared under dry conditions, using silica reagents (such as tetraethylorthosilicate, TEOS) which were finally

hydrolyzed and calcined.[65] In Figure 9, the XRD patterns and the structure of the different MWW derivative materials obtained from the layered zeolitic precursor are shown to finally give the pillared MCM-36 zeolite. It is remarkable that the interlayer separation achieved with the swelling process was maintained after the insertion of silica pillars.[66]
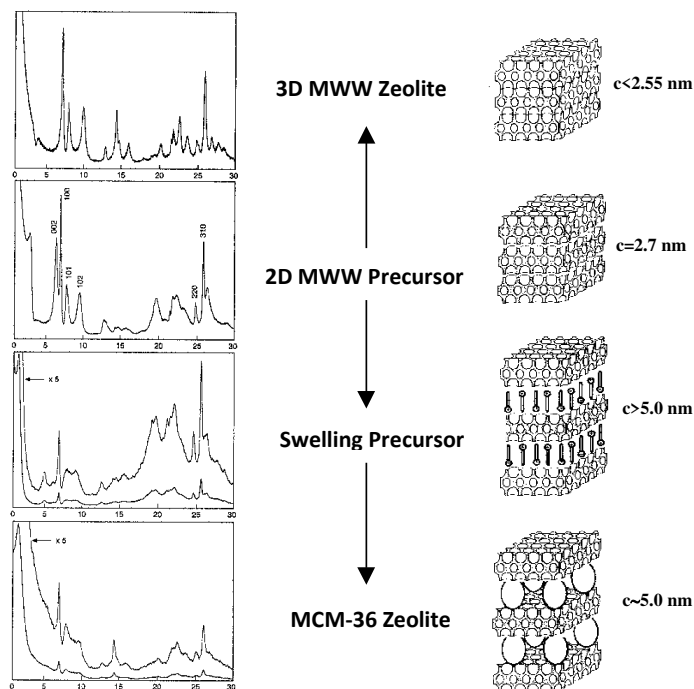

Figure 9. Scheme of pillared MCM-36 zeolite and XRD patterns associated to MWW derivative materials obtained through pillarization process (according to reference 66).

In Figure 10, a scheme of the pillared MCM-36 zeolite is given. In this scheme it is evidenced that the 10MR sinusoidal channels into the MWW zeolitic layers remain un-modified. On the contrary, the delimited 12MR super-cages, which are formed after the linkage of the MWW layers, are not formed after the pillarization process, and a new type of mesoporous cavities are generated, which exhibit between 2.5 nm and 3.0 nm pore diameter, due to the effective intercalation of silica pillars. As a consequence of the pillarization, the BET surface area obtained for MCM-36 is strongly increased compared with the microporous MCM-22 zeolite. The mean advantage of the mesoporous distribution generated in the MCM-36 was the easy accessibility achieved to internal acid active sites, overall for voluminous reactant molecules which take part in the catalytic reaction.[67, 68] On the contrary, the pillared materials, such as the MCM-36 zeolites, show the important inconvenient associated to the partial blockage of active sites, present in the external surface of MWW layers, due to the intercalation of silica pillars in the interlayer space.[69] Similarly, pillared zeolitic materials, denoted as ITQ-36[70] and MCM-39,[71] were also obtained from PREFER and Nu-6(1) layered precursors, respectively, using both silica and metallic oxides as pillaring agents.
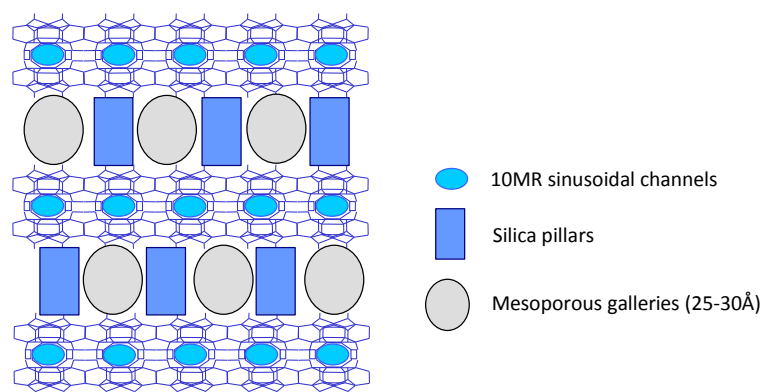
Figure 10. Artistic representation of pillared MCM-36 zeolitic materials.

Pillars formed by oxides other than silica can even supply additional active sites. In this way, magnesia–alumina were used for pillaring the MWW layered zeolitic precursors, obtaining MCM-36 materials with significantly higher mesoporosity (pore size diameters between 2–4 nm) compared with the use of only alumina as structural pillars.[72] Furthermore, other mixed oxides were also used as pillaring agents, such as BaO–Al$_2$O$_3$, Al$_2$O$_3$–SiO$_2$, MgO–Al$_2$O$_3$–SiO$_2$ and BaO–Al$_2$O$_3$–SiO$_2$, synthesizing ordered zeolitic pillared materials with additional mesoporous interlayered galleries.[73] These MWW pillared materials could even be considered as acid-base bi-functional materials which would contain enhanced Lewis and Brönsted acidity, generated by pillaring with aluminum oxides and/or silica-alumina clusters, and base properties by the incorporation of alkaline earth oxide aluminates (MgO/BaO-Al$_2$O$_3$), both located between the zeolitic layers in the interlayered space.[74]

The strong alkaline conditions and high temperatures normally used during the swelling process normally carried out could favor the disruption of the MWW layered structure and the partial dissolution of the highly siliceous zeolitic sheets to form standard mesoporous M41S-type materials. To avoid this problem, Tsapatsis *et al.* employed milder conditions in the swelling step, working meanly at room temperature. This modified approach to swell MWW zeolitic precursors allowed to prepare pillared MCM-36 and also partially exfoliated materials conformed by well-defined MWW layers which preserve their morphology and crystalline structure (Figure 11).[75] These MCM-36 derivatives with bimodal meso- and microporous nature, synthesized under milder conditions, were used as catalysts for ethanol dehydration and monomolecular conversion of propane and isobutene, considered as test reactions. The results corroborated that the rate and the activation energy in zeolites, possessing dual porous nature, were comparable to conventional microporous 3D-MWW materials, implying this fact that, in pillared zeolites, the catalytic behavior of Brönsted acid sites is preferentially dominated by the microporous environment because it provides a better fit for adsorption of small alkane or alcohol substrates.[76]
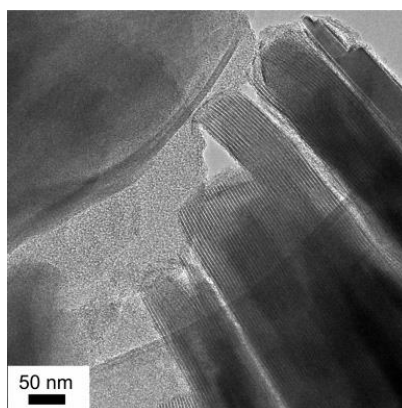
Figure 11. TEM image of MCM-36 obtained from MWW precursors swollen at room temperature (according to reference 75).

Conventionally, the microporous structure of zeolites favors high selectivities when they are used as catalysts due to the presence of uniform pores sizes and channels. However, this also implies important diffusivity constraints for reactants, intermediate compounds and products. So, the use of zeolites with improved accessibility, while preserving their intrinsic zeolitic activity as it occurs with pillared zeolites, would facilitate chemical catalytic processes where compounds with larger molecular sizes take part.[77] This can be seen when using MCM-36 with molybdenum or nickel species for methane non-oxidative aromatization[78] or ethylene oligomerization,[79] respectively. Also, vacuum gasoil cracking,[68] alkylations of biphenyl or benzene with propylene[80, 81] or phenol by *t*-butanol[82, 83] in gas phase and liquid phase, respectively, were performed using pillared MCM-36 zeolites. In this last example, the results confirmed the decisive contribution of the accessible acid sites located at the external surface of MWW layers, being the diffusion of the bulky compounds inhibited inside the microporous sinusoidal 10 MR channels present in the intralayer.

Similar conclusions were achieved by Fajula *et al.* for the conversion of methanol to hydrocarbons (MTH) catalyzed by MCM-36 zeolites where the diffusion of bulkier species is facilitated with the use of more accessible pillared mesoporous catalysts, resulting in lower deactivation rate compared with the microporous 3D MCM-22 catalyst.[84] Additionally, MCM-36 materials were confirmed as excellent catalysts for bulk chemical processes related with *in-situ* reduction of NO_x from fluid catalytic cracking units (FCC), developing more sustainable chemical processes.[85]

Recent advances, in the pillarization concept, have allowed achieving multifunctional hybrid organic-inorganic catalytic materials with a hierarchical system of well-defined micro- and mesopores, obtaining similar bimodal porous zeolites that those prepared from natural layered aluminosilicates or preformed zeolite nanoparticles used as precursors.[86] In this case, they have been prepared from MWW zeolitic precursors by intercalation and stabilization in the interlayer space of amino-aryl-bridged silsesquioxanes, so-called disilanes, between inorganic zeolitic layers (see Figure 12). The organic linkers are conformed by two condensed silyl-arylic groups from disilane molecules, such as 1,4-bis(triethoxysilyl)benzene (BTEB), which react with the external silanol groups of the zeolitic layers. This type of hybrids (MWW-BTEB) contained micropores within the inorganic MWW layers and a well-defined mesoporous system between the organic linkers. An amination post-treatment introduced base groups in

the organic linkers close to the acid sites present in the structural inorganic counterpart due to the presence of framework aluminum. Through this methodology it has been possible to prepare bi-functional acid-base catalysts where the acid sites, of zeolitic nature, are located in the inorganic building blocks and the base sites are part of the organic structure (Figure 12). The resultant materials acted as bi-functional catalysts for performing a two-step cascade reaction that involved the hydrolysis of hemi-acetals followed by Knoevenagel condensation processes, in line with C-C bond formation reactions type.[87]
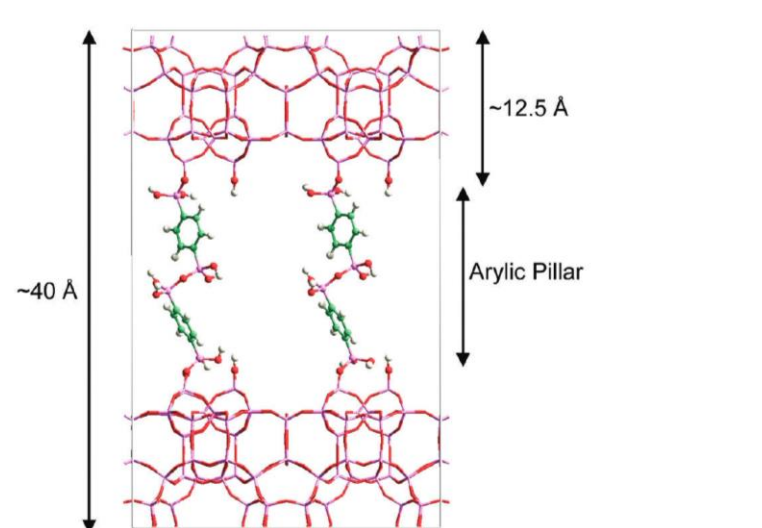

Figure 12. Artistic representation of layered hybrid material obtained by pillaring with BTEB silsesquioxane molecules (according to reference 87).

Related with pillared materials, Tatsumi *et al*. prepared a novel type of stabilized interlayer-expanded MWW zeolitic materials, named IEZ-MWW. The synthesis was made by intercalation of monomeric silica puncheons between the zeolitic sheets, acting as small pillars conformed by only one silicon atom. $SiMe_2Cl_2$ or $Si(EtO)_2Me_2$ were generally used as stabilizer agents which reacted with the external surface silanol groups. This allowed the generation of derived MWW materials with additional 12 MR microporous channels between the inorganic layers in which the strong acidity of zeolitic nature was preserved (Figure 13). This silylation synthesis allowed more accessible porosity to the prepared materials. Currently, vapor-phase silylation has also been used to obtain this type of IEZ-MWW layered materials.[88] This methodology to obtain expanded lamellar zeolites has also been applied to other layered zeolitic precursors, above considered, conformed by ferrieritic or CDO individual sheets (Table 1).[89]
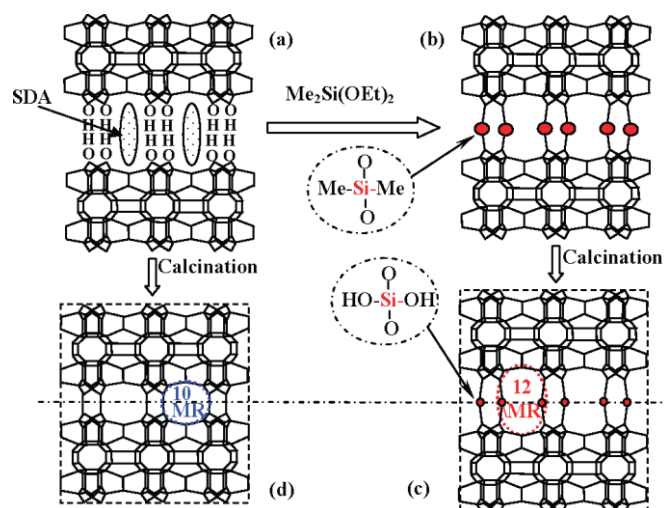
Figure 13. Synthesis route to obtain IEZ-MWW materials by post-synthesis treatments using dialkoxysilylated precursors (according to reference 89).

Additionally, tetrahedral titanium coordinated into the network of each MWW layers of the expanded zeolites has also been introduced by the previous synthesis of Ti-MWW precursors in presence of boron sources, such as it was discussed in the previous section.[90] When acid post-treatment processes were carried out on these Ti-MWW precursors to effectively remove the extra-framework octahedral Ti species, a structural modification was observed, obtaining a novel 3D titanosilicate denoted Ti-YNU-1.[91] This zeolitic material showed a more expanded pore window between the crystalline MWW sheets, similar to IEZ-MWW solids, due to the generation of two additional T sites in the interlayer space, favoring a cell expansion in the *c* direction by the formation of further interlayered 12 MR channels. In this case, it was hypothesized that Ti centers could occupy the pillar sites, having a higher steric accessibility than when they were in network positions in conventional 3D MWW or TS-1 materials, being effective as active centers for olefins' epoxidations (Figure 14).[92] These acid post-synthesis treatments and the reversible structural conversion from MWW precursors, above exposed, could be applicable to the preparation of other metallosilicates for different catalytic applications.[93]
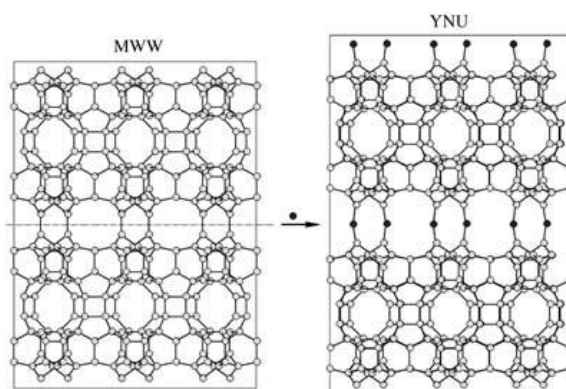

Figure 14. Schematic transformation of Ti-MWW and Ti-YNU-1 materials (according to reference 91).

2.3- Delaminated or exfoliated zeolites

Advances in the preparation of more accessible zeolitic materials, from inorganic bi-dimensional layered precursors, were achieved by generating novel materials where the practical totality of the zeolite surface is transformed to accessible external area. For this, the zeolitic layered precursors are involved in *delamination* or *exfoliation* processes with the objective to completely separate the piled ordered layers in a random distribution of the individual inorganic sheets (Figure 1).[94] The exfoliated zeolitic materials with very high external surface areas exhibit high accessibility for reactants with large molecular size which can easily interact with the active sites at the surface of each inorganic zeolitic sheet. Moreover, the high external area characteristic of *delaminated materials* can be used to incorporate different active sites which are stabilized and separated at controlled distance onto the surface of the layers, or to generate multifunctional catalysts. These materials show the advantages of mesoporous materials combined with the hydrothermal stability characteristic of zeolitic solids.

It is important to remark that although the delaminated materials are formed by disordered zeolitic layers, they are not amorphous, being formed by well-structured single layers of zeolites. We will show that by optimization of the delamination process, the final characteristics of the exfoliated solids can be controlled.

2.3.1 ITQ-2 delaminated zeolite and related materials

The first delaminated (single layer) zeolitic material reported was named ITQ-2.[95] This solid is formed by randomly separated individual MWW layers of, approximately, 2.5 nm of thickness, exhibiting a high external and accessible surface area (>700 m^2g^{-1}). The nanolayers are structured by a hexagonal distribution of cups present in both sides of the zeolitic sheets. These calices-type are delimited by 12 MR, showing an outer aperture of ~(0.7 x 0.7) nm and being connected with the cups of the opposite side, into the same MWW layer, through the double 6 MR with a hexagonal prism conformation. Additionally, sinusoidal channels delimited by 10 MR are present around the cups, along the plane *ab* of each individual MWW layer (Figure 15). The delaminated ITQ-2 preparation method is based in the swollen, exfoliation and calcination of the MWW layered zeolitic precursors, being the delamination step carried out using ultrasonic techniques or other mechanical processes, such as for instance continuous and vigorous stirring (Figure 16).[96]
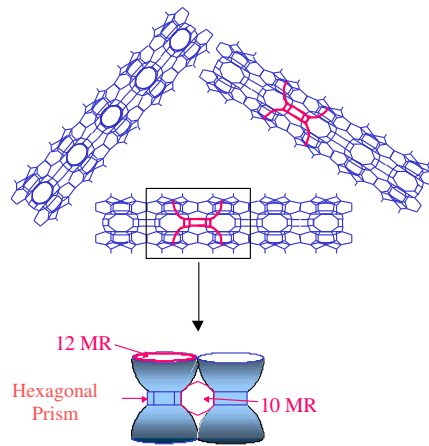
Figure 15. Artistic representation of the ITQ-2 delaminated zeolite (according to reference 96).
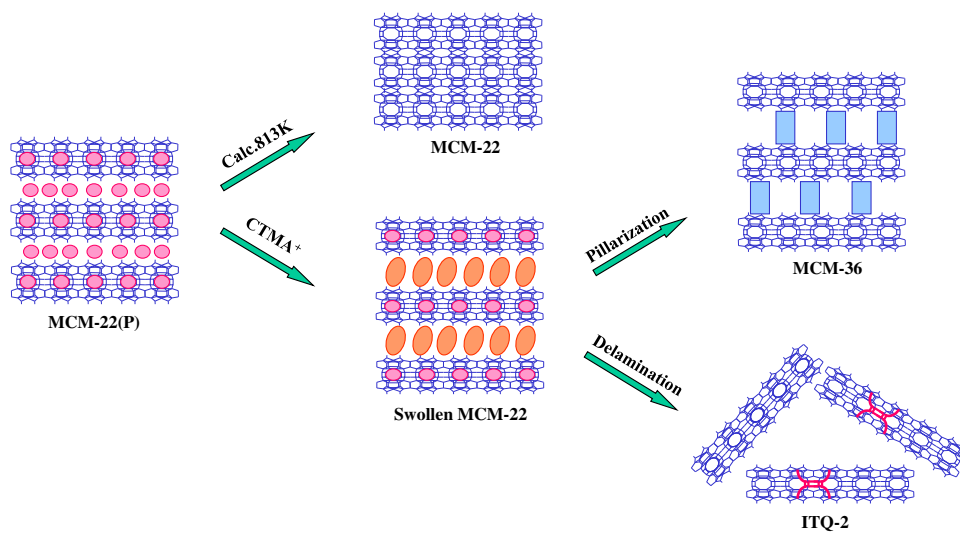

Figure 16. Preparation scheme to prepare ITQ-2-type delaminated zeolites (according to reference 96).

It is possible to follow the delamination process from X-ray spectroscopy of the starting layered zeolitic materials (Figure 17).[68] Specifically, ITQ-2 pattern does not show the *(001)* and *(002)* peaks at 2Θ = 3-7º which is consistent with the proposed structures; that is, ITQ-2 does not have the regular array of layers, with its characteristic 2.5-nm periodicity, typical of the MWW topology.[97] Comparing the X-ray diffraction patterns of ITQ-2 with that of MWW-type zeolite of similar silica-to-alumina ratio reveals that the high angle peaks are much broader for ITQ-2, which is indicative of a reduction in the size of the domain of coherent scattering; that is, exfoliation of the MCM-22(P) has significantly reduced the long range order in the ITQ-2 structure.[98]
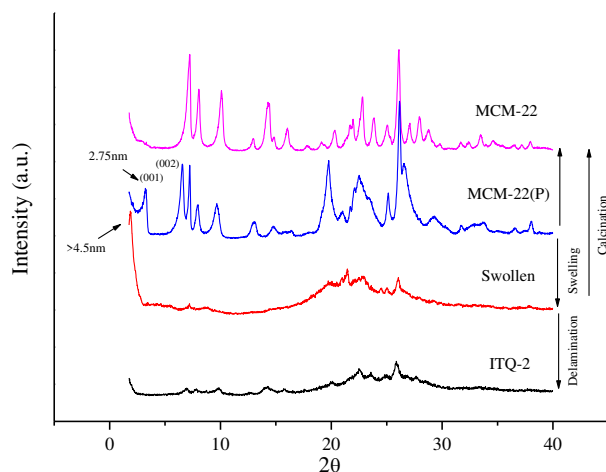
Figure 17. X-ray patterns of the layered MWW materials obtained during the preparation of ITQ-2-type delaminated zeolites (according to reference 98).

The structural characteristics of delaminated ITQ-2 zeolites were corroborated from high resolution transmission electronic microscopy (HR-TEM) through the identification of the MWW individual nanosheets (Figure 18). It is possible to distinguish between the regular arrays of exposed 0.7 x 0.7 nm cups and the 10-ring channel system in between them when the layers are parallel to the microscopes' optical axis (Figure 18a). In this case, the observed disorder is an intrinsic property of the ITQ-2 materials. TEM image of the MWW-type zeolite is shown in Figure 18b for comparison, clearly showing the bonding of cups to form super-cages. In general, all characterization results confirmed that delaminated ITQ-2 materials exhibited the properties corresponding to highly accessible zeolitic structures formed by individual MWW layers with a random spatial distribution, combining the acidity and hydrothermal stability characteristic of conventional zeolites with the high accessibility to voluminous molecules typical of the mesoporous silicates.[99]
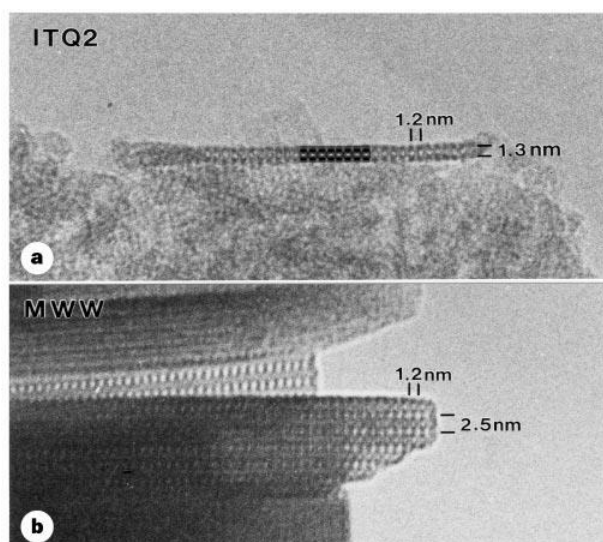

Figure 18. TEM micrographs of (a) ITQ-2 and (b) 3D MWW zeolites (according to reference 96).

If too strong alkaline conditions are employed during the delamination process, in the swelling step, partial dissolution of MWW zeolitic layers may occur, and this should be taken into account to optimize the delamination process. Then, studies were carried out trying to

17

obtain well-defined delaminated ITQ-2 zeolites using milder conditions. Following this scope, Zones *et al.* have synthesized another material so-called UCB-1 which was obtained through the delamination of zeolitic MWW layered precursor, such as in the standard ITQ-2, at pH 9 using an aqueous solution of cetyltrimethylammonium bromide, tetrabutylammonium fluoride, and tetrabutylammonium chloride. For this, fluoride anion is used because it is an established reagent for the deprotection of silyl ethers and is known to form strong interactions to Si(IV) cations. Furthermore, chloride was used because it is an aggressive anion for rusting anodized aluminum. So, the authors concluded hypothesizing that delamination can be successfully conducted using a mixture of fluoride and chloride anions.[100] Indeed, the characterization results evidenced similarities between UCB-1 and the previously reported delaminated ITQ-2 materials. However, the external surface area finally measured in the UCB-1 materials is close to that of standard 3D MWW zeolites, which would be indicative that the disorder achieved with this methodology is reduced. Probably, UCB-1-type solid is formed by crystalline units structured each one by several packed MWW layers, generating a partially delaminated zeolite. Specifically, this methodology was based in exfoliation processes through chemical deprotection steps, involving breaking of Si-O and Al-O bonds in the interlayer region.

Tatsumi *et al.* prepared Ti-MWW layered precursors, combining acid extraction and deboronation processes with the assistance of cyclic amine through post-synthesis treatments. So, delamination routes applied on Ti-MWW lamellar precursors allowed to obtain a new type of titanosilicate, so-called Del-Ti-MWW, with tetrahedral titanium presents into the framework of the individual MWW zeolitic layers that was incorporated directly during the synthesis process, being useful as catalyst for epoxidation of alkenes with various molecular sizes. The success of the delamination process was completely confirmed from TEM images which showed crystalline materials conformed by fewer sheets than 3D Ti-MWW, being even possible to appreciate single MWW sheets (Figure 19).[101] This method could be an alternative to incorporate active tetrahedral titanium into the framework of MWW layers, avoiding post-grafting steps to covalently incorporate, in the external surface, active titanium complexes such as titanocene.[102, 103, 104] However, there is an alternative to this method to produce Ti-ITQ-2 starting from Ti-ITQ-1.[105]
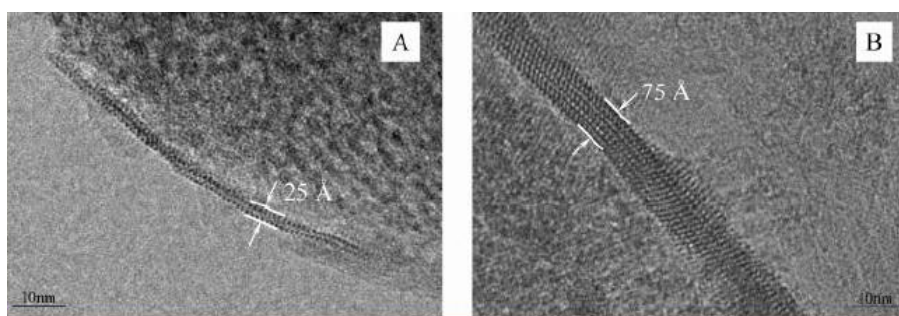
Figure 19. HRTEM micrographs of single sheet (A) and pack of three sheets (B) of Del-Ti-MWW (according to reference 101).

Efforts have been made to obtain exfoliated MWW materials directly during the hydrothermal synthesis, avoiding the post-synthesis alterations of layered zeolitic precursors through swelling and delamination steps. Following this approach, MCM-56 zeolite, with similar structure to MCM-22, was obtained directly during the synthesis processes, such as MCM-49, by modification of alkaline and cyclic imines concentrations introduced in the

synthesis slurry.[106] However, although in this zeolite it is observed a partial disordered organization due the presence of curved packs of MWW sheets which provided some higher external surface area, it is not possible to consider MCM-56 as a delaminated zeolite with total exfoliation of the MWW layers.[107] Indeed, the external surface area of MCM-56 is far from that of ITQ-2 and from the theoretical values of external surface area that are expected from delaminated MWW materials.[98] Recently, Corma *et al.* have prepared a zeolite (ITQ-30) structurally similar to MCM-56, by high-throughput synthesis techniques and using N(16)-methyl-sparteinium as SDA.[108] Similarly, Roth *et al.* have reported a new member into the MWW group, so-called EMM-10, in which the layers are stacked without vertical alignment, using diquaternary ammonium molecules as template.[109] In these cases, the structural analysis carried out with MCM-56, ITQ-30 and EMM-10 layered zeolites showed that they are similar, being only differenced by slight modifications in the spatial organization of the piled MWW layers which are perpendicularly disposed to axis *c*.

Exfoliated ITQ-2 zeolites and derivatives can be used directly as acid, base and bi-functional catalysts when substrates with large molecular sizes have to be reacted. This fact was evidenced by means of catalytic-cracking tests, using n-decane and vacuum gasoil, and cumene or 1,3,5-tri-isopropylbenzene dealkylation, being observed that delamination processes favored the preparation of more accessible heterogeneous catalysts for bulky molecules, maintaining the characteristic zeolitic acid strength in their active sites.[95, 98, 110] Following this line and considering the high surface area, the acid site's accessibility and the hydrothermal stability of ITQ-2 zeolites, elevated yields were obtained for skeletal isomerization and dehydroisomerization of 1-butene and n-butene to isobutene or alkylation of toluene with methanol and biphenyl with propylene, avoiding in both cases the extensive coke formation.[111, 112, 113]

The physico-chemical and textural properties linked to highly accessible delaminated ITQ-2 zeolites were also positive to carry out reactive processes with industrial application such as the synthesis of diaminophenylmethane (DADPM), *i. e.* the polyamine precursor in the production of methylene diphenylene diisocyanate (MDI) for polyurethanes generation.[114, 115, 116] Moreover, the open structure of exfoliated materials was used for methanol to olefins conversion (MTO) and dehydrogenation of propane to propylene in presence of CO_2 over ITQ-2 supported gallium oxide.[117, 118]

ITQ-2 also gave excellent results for hydrocracking, and for hydrotreating light cycle oil (LCO) fractions, being the MWW delaminated catalysts supported with Ni-Mo and Pt species excellent for mild hydrocracking (MHC) of vacuum gas oil and aromatic hydrogenation due to the combination of the efficient activity of zeolites with the desired selectivity of metallic catalysts.[119, 120] Additionally, uniform cobalt particles were incorporated onto MWW layers of silylated ITQ-2 zeolites, through reverse-micelle synthesis methodology, generating improved catalysts for Fisher-Tropsch synthesis (FTS).[121, 122, 123] This catalytic Co-ITQ-2 system was also useful for the direct conversion of syngas to high-octane gasoline-range hydrocarbons by the conventional FTS process, the highest yields of branched gasoline products being exhibited by the ITQ-2 derivatives with the largest surface area.[124] Inside of the delaminated MWW catalysts obtained from the incorporation of metallic nanoparticles, bi-functional ITQ-2 materials were prepared combining Brönsted acidity due to framework aluminum with the presence of Mo species onto external surface, being efficiently used for methane

dehydroaromatization (MDA) reaction.[125] Also, exfoliated catalysts based on Ni and Co nanoparticles, supported on purely siliceous ITQ-2, were successfully used for bioethanol steam reforming.[126]

The high accessibility and zeolitic acid strength of ITQ-2 have expanded the possibilities of zeolites for catalytic applications into the field of fine chemicals preparation as demonstrated in our group. [127] For instance, during the preparation of dimethylacetals and tetrahydropyranylation of alcohols and phenols, it was shown that when bulky reactants are involved in the reaction, ITQ-2 exhibited higher activity than large pore zeolites due to the optimal combination of strong and accessible acid centers.[128, 129] Acetalization reactions on ITQ-2 conducted very successfully to the synthesis of orange blossom and apple fragrances. Similarly, direct synthesis of phenylacetaldehyde glycerol acetal and vanillin propylene glycol acetal, which are flavoring compounds with hyacinth and vanilla scent fragrances, respectively, were successfully performed by acetalization of phenylacetaldehyde and vanillin with glycerol and propylene glycol, using exfoliated MWW materiasls as catalysts in environmentally friendly process.[130, 131]

Non-steroidal drugs, with anti-inflammatory and analgesic activities, were synthesized, in presence of ITQ-2 zeolite, by the oximation of acetophenone derivatives followed by the solid acid-catalyzed Beckmann rearrangement to give corresponding amides.[132, 133] Additionally, Diels-Alder and retro-Diels-Alder reactions between cyclopentadiene and *p*-benzoquinone, Prins condensations of β-pinene with paraformaldehyde for Nopol production, and aqueous phase dehydration of xylose to furfural, were carried out with delaminated ITQ-2 materials where accessible acid sites were stabilized by the zeolitic network.[134, 135, 136]

Taking advantage of the elevated external surface area and the presence of high concentrations of accessible and reactive silanol groups onto individual MWW layers, ITQ-2 delaminated materials were also used to covalently incorporate other organic active species. In this way, organocatalyst compounds were incorporated, generating organic-inorganic hybrid materials with catalytic applications, overcoming the limitations imposed by the organic soluble catalysts, *i. e.* stability, recovering and recycling. This is the case for the incorporation of heterogenized porphyrins and metaloporphyrins on robust solids such as purely siliceous ITQ-2 zeolites, generating active electrocatalysts for oxygen reduction processes with reduced activity lost due to the minimized desorption of active complexes.[137]

Following this anchoring approach, Schiff bases complexes were stabilized onto MWW individual layers from ITQ-2 delaminated zeolites, generating active asymmetric catalysts for enantioselective epoxide ring opening reactions when grafted chromium salen complexes were incorporated. [138] Similarly, chiral delaminated ITQ-2 zeolites were formed by anchoring stabilized salen (Pd and Ni) complexes, being effectively used (TOFs around 200×10^3 h^{-1}) to catalyze the hydrogenation of imines or alkenes,[139, 140] and for Heck and Suzuki coupling reactions under phosphine-free conditions.[141] Inside this line, epoxidation of several prochiral alkenes was favored by grafting Mn(II) salen complexes onto delaminated ITQ-2 support zeolites through axial coordinating ligands.[142] Moreover, strong increase of the enantioselectivity was obtained after the post-synthesis silylation of the external free silanol groups located in the individual MWW sheets of ITQ-2 materials for the reaction of aldehydes with trimethylsilyl cyanide to obtain the corresponding cyanohydrins.[143] However, not only

chiral salen complexes were effectively anchored on ITQ-2 to generate chiral catalysts, pre-fixed chiral triaza ligands onto MWW layers allowed the final incorporation of Pd, Rh or Ir complexes which were active for olefin hydrogenation reactions.

Furthermore, anchored systems based on chiral amines, containing pyrrolidine backbones, were useful to obtain active and recyclable catalysts for Michael additions of acid esters to acrolein.[144] Interestingly, mononuclear NHC carbine-gold complexes were also covalently grafted on delaminated ITQ-2 zeolite for hydrogenation of alkenes and for Suzuki cross-coupling reaction, yielding selectively non-symmetrical biaryls.[145] Related with this last approach, Au(I) and Pd(II) complexes were heterogenized onto ITQ-2, obtaining effective catalysts for Sonogashira cross-coupling reactions between iodobenzene and arylboronic acids or alkynes.[146] Stabilized enzymes were also covalently supported onto MWW layers which are forming ITQ-2 zeolites, generating novel biocatalysts.[147]

The benefits of the open zeolitic structures, derived from MWW layered precursors, can be exploited in other catalytic fields, more related with electro- or photo-catalysis. For instance, it is important the generation of electron transfer species with high stability and durability. In this way, the prevalence of the external surface over the internal porosity in the delaminated ITQ-2 zeolites favors the spontaneous generation and stabilization of radical cations. Then, photoinduced electron transfer species were also produced after the treatment of ITQ-2 zeolites, with previously immobilized $Ru(bpy)^{32+}$, methylviologen or blue light-emitting hydroxyquinolinate ligands onto the external cups, through emission and time-resolved laser flash photolysis.[148, 149, 150, 151,152] Alternatively, exfoliated MWW materials were also used as sensors by the covalent grafting of fluorophere compounds , such as pyrene, generating selective heterogeneous sensor for iodide in the presence of other halides in the reaction media.[153] Moreover, ITQ-2 zeolites were successfully used to adsorb and capture gases, such as CO_2 or SO_2, after the post-functionalization by external anchoring of MWW individual layers with pending amino groups. [154, 155, 156]

2.3.2 ITQ-6, ITQ-18 and ITQ-20 delaminated zeolites

ITQ-6,[157] ITQ-18[158] and ITQ-20[159] delaminated zeolites were also obtained from PREFER, Nu-6(1) and ITQ-19 zeolitic precursors (Table 1), respectively, following similar preparation routes as for ITQ-2 (see Figure 16). Specifically, ITQ-6 is formed by disordered ferrieritic layers with ~0.9 nm of thickness, being each zeolitic sheet structured by an assembly of 5 MR pentasils linked between them (Figure 20).[160] At the external surface of each FER layer, there are small cavities with ~(0.28x0.42) nm of internal diameters because the microporous channels delimited by 10MR, present in the 3D Ferrierite, are not formed in the delaminated ITQ-6 zeolites.
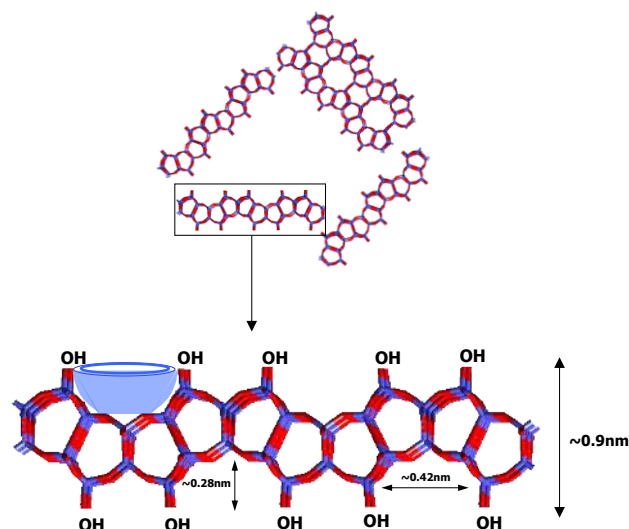
Figure 20. Representation of delaminated ITQ-6 zeolite, showing detail of individual ferrieritic layer.

The possibility to synthesize Ti-PREFER was explored since this layered precursor is prepared in fluoride medium. Exfoliated ferrieritic ITQ-6 materials with tetrahedral titanium (Ti-ITQ-6) were obtained, being effective catalysts for epoxidation of olefins with H_2O_2.[44, 161] The elevated external surface area ($\sim$500 m^{2}g^{-1}) and the associated high accessibility present in these type of zeolites also allowed anchoring different active organocatalysts, such as organometallic complexes[141] or even enzymes by covalent or electrostatic immobilizations, avoiding the rapid deactivation of supported biocatalysts in penicillin hydrolysis reactions and increasing the enzymatic stability (Figure 21).[162, 163] Moreover, the ITQ-6 supporting matrixes were recycled and reused to immobilize further enzymes.[164] The optimal characteristics of delaminated ITQ-6 materials as effective stable supports were also evidenced when vanadia was incorporated and homogeneously dispersed onto ferrieritic layers. In this case, active catalysts for oxidative dehydrogenation of propane were obtained, exhibiting high yields to propylene.[165] Alternatively, milder non-aqueous conditions using fluoride/chloride anionic mixtures were also effective to promote delamination of layered precursors formed by ferrieritic layers.[166]
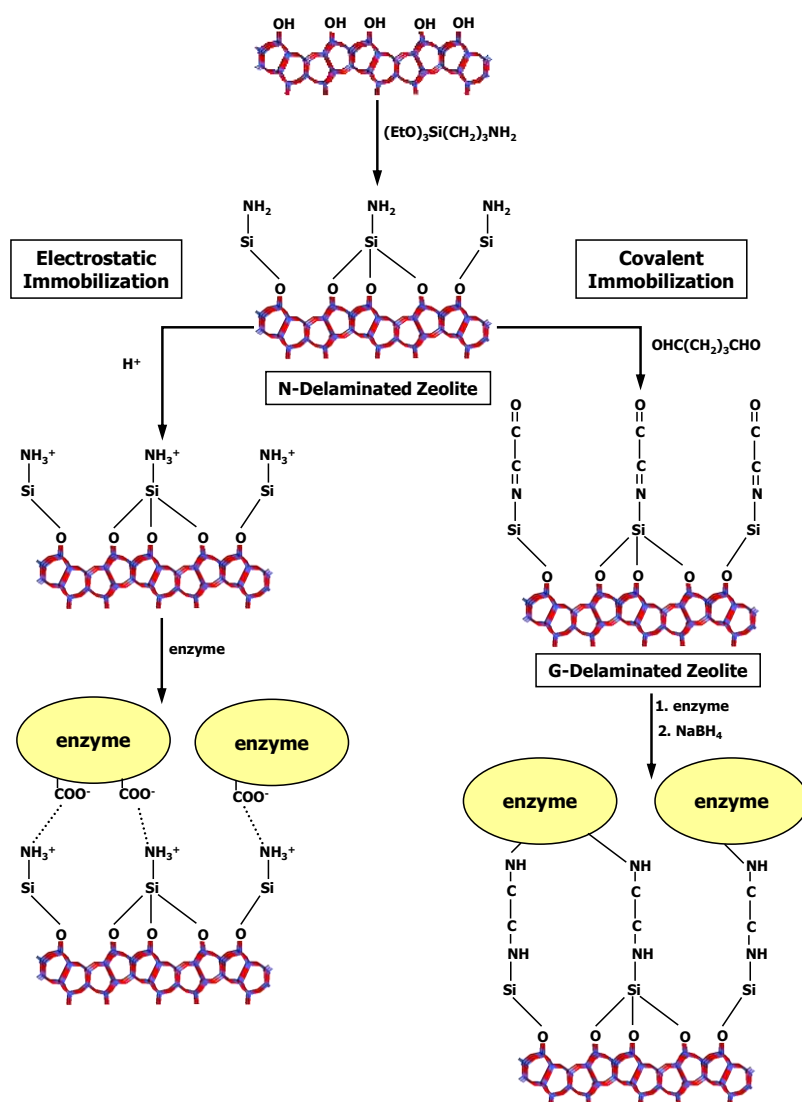
Figure 21. Immobilization of enzymes onto delaminated ITQ-6 zeolites used as inorganic supports.

3- Direct synthesis of layered materials based on zeolitic single structural units

Up to now, we have described the preparation of mono-layered zeolites derived from reported lamellar precursors. Furthermore, we have presented the pioneering reports showing the clear benefit of the mono-layered delaminated zeolites for acid catalysis, as support for metals and oxides to generate mono- or bi-functional catalysis, for supporting transition metal complexes or enzymes, or for photochemical applications. The combination of zeolitic properties with high external surface area and site accessibility of the delaminated mono-layered zeolites, with the corresponding exceptional properties, prompted to researchers to attempt the direct synthesis of those materials. Recently, Ryoo *et al.* have prepared a novel family of layered materials based on zeolitic nanosheets due to the use, during the zeolites' hydrothermal synthesis, of specific dual structural directing agents (SDAs) with surfactant characteristics. Then, hydrothermal synthesis conditions, in presence of diquaternary ammonium bi-functional surfactants, allowed obtaining stable single-unit-cell nanosheets of zeolite MFI (Table 1).[167]

Specifically, the organic molecules $C_{22}H_{45}$-$N^+(CH_3)_2$-C_6H_{12}-$N^+(CH_3)_2$-C_6H_{13} (normally so-called C_{22-6-6}) were used as ammonium-type surfactants. This SDA compounds were composed of a long-chain alkyl group (C22) and two quaternary ammonium groups spaced by a C6 alkyl linkage. The diammonium head group acted as an effective structure-directing agent for the MFI zeolite nanocrystal, while the hydrophobic interaction between the long chain branches favored the formation of micellar ordered or non-ordered lamellar organization. With the use of this type of surfactants, an ultrathin like-nanosheet zeolite framework of only 2 nm thick was formed at the hydrophilic part of the micelles, while the hydrophobic branches limited the natural growth of zeolites crystals (Figure 22). Interestingly, it was detected that modifying the synthesis conditions, particularly sodium concentration, ordered multi- or uni-lamellar solids were obtained by regular stacking, along *b*-axis, or random spatial distribution of MFI nanosheets, respectively. The elevated number of accessible acid sites on the external surface of these zeolitic MFI layers implied that they were highly active for the catalytic conversion of large organic substrates, the reduced crystal thickness easing the molecules diffusion and thereby strongly reducing catalyst deactivation by coke formation during the methanol-to-gasoline process.
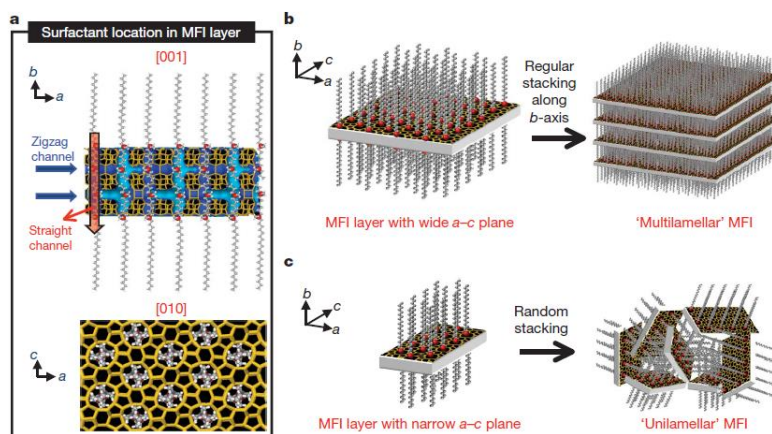

Figure 22. Scheme of single MFI nanosheets crystallization (a). MFI nanosheets form either multilamellar stacking along the *b*-axis (b) or a random assembly of unilamellar structure (c) (according to reference 167).

Such as it was reported, the ammonium heads acted as a structure-directing agent for the microporous MFI zeolite, while the surfactant tails facilitated the auto-assembled versus a layered micellar organization. The two types of structural effects were investigated by using several surfactant molecules with different spacers between ammonium heads and tails with variable linear alkyl length. The results obtained concluded that the bi-functional surfactant molecules equipped with at least two suitable ammonium groups were optimal for the crystallization of MFI zeolite structure. Moreover, the thickness of the nanosheets was increased and controlled in function of the number of the head ammonium groups (Figure 23). All these considerations, about the surfactant characteristics, could be useful for *a priori* design hierarchical zeolites formed by crystalline layers.[168]
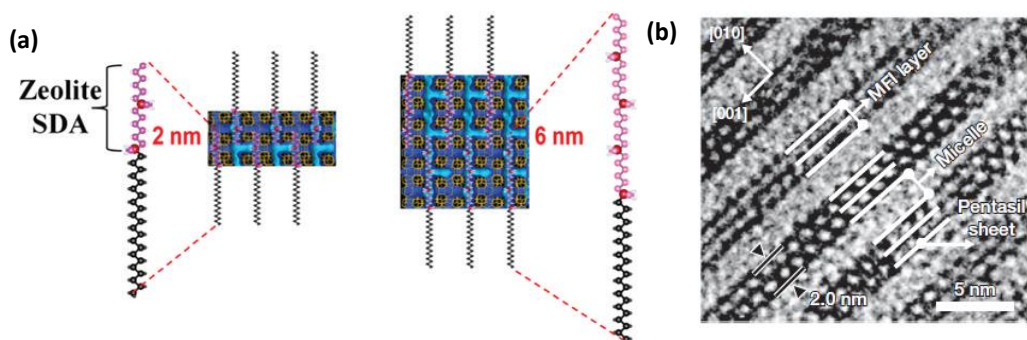
Figure 23. (a) Schematic representation of lamellar MFI materials prepared with bi-functional surfactants with different number of head ammonium groups. (b) TEM cross-section of lamellar MFI zeolite, showing that each plate is composed of lamellar stacking of consecutive layers of MFI (2 nm) and surfactant micelle (2.8 nm). The MFI layer is composed of three pentasil sheets, corresponding to the thickness of a single unit cell dimension along the b-axis (according to reference 167 and 168).

Advancing along this synthesis approach based on the use of dual structure-directing agents, gemini-type triammonium surfactants, $[C_{18}H_{37}–N^+(CH_3)_2–C_6H_{12}–N^+(CH_3)_2–C_6H_{12}–N^+(CH_3)_2–C_{18}H_{37}][Br^-]_3$, were used, successfully generating zeolite nanosheets with an extremely thin thickness of MFI zeolite crystals of only 1.5 nm in the *b*-direction. These nanosheets were thinner than a single crystal unit-cell of 2.0 nm thickness along the *b*-direction, above commented (Figure 24). This type of zeolite sample was so-called as SPZ for "Single Pore Zeolite". Furthermore, in function of the basic conditions used, multi-lamellar ordered or uni-lamellar non-ordered MFI zeolites were also prepared. As can be expected from previous results with delaminated zeolites,[96] SPZ materials exhibited high acid catalytic activity for the conversion of bulky molecules.[169]
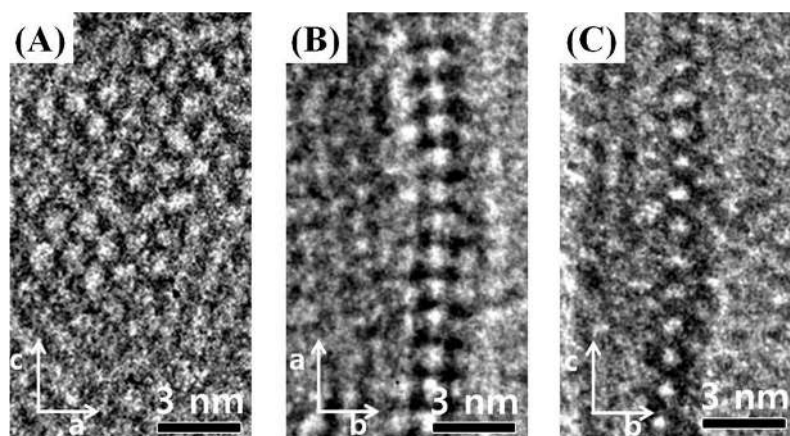

Figure 24. TEM images of a 1.5 nm thick zeolite nanosheet projected down the [010] (a), [001] (b) and [100] (c) crystallographic axes (according to reference 169).

As showed before with layered zeolites, the direct synthesis of multi-lamellar ordered MFI zeolites, as layered zeolitic precursors, allowed their post-synthesis modifications to generate pillared or delaminated solids formed by MFI nanosheets with different spatial distribution. In the case of pillarization process, the mesoporous volume present in the interlamellar space was retained by separating the zeolite layers with silica pillars even after surfactant removing by calcination step. Moreover, the diameters of these mesoporous

galleries generated were tuned in function of the surfactant tail lengths (Figure 25).[170] Analyzing in detail the zeolite structure generation process of multi-lamellar MFI materials, it was elucidated that the MFI nanosheets were initially obtained as a disordered assembly that was transformed into an ordered multi-lamellar mesostructure by dissolution-recrystallization consecutive steps, during the hydrothermal synthesis. When several synthesis parameters, which affect the rates of the initial formation of nanosheets and their posterior restructuration process, were investigated (such as temperature variation, structure of the surfactant tail, molar ratio of synthesis compounds and basicity concentration), it was possible to synthesize stabilized exfoliated zeolites based in disordered MFI nanosheets. These solids exhibited large mesopore areas and volumes such as were observed for delaminated zeolites ITQ-2 and ITQ-6.[171]
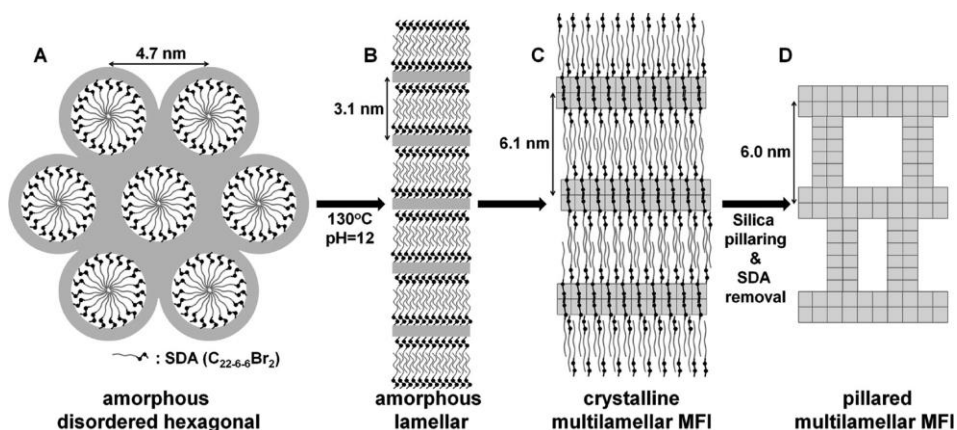

Figure 25. Scheme of phase transformation during the hydrothermal synthesis of multi-lamellar MFI zeolite using bi-functional diquaternary ammonium surfactants and its consecutive pillaring process (according to reference 170).

With the objective to explore the catalytic possibilities of lamellar MFI zeolites, the nature of acid sites located in the structure of this type of zeolites was profusely analyzed. Specifically, distribution, acid strength, and steam stability of internal and external acid sites were studied for zeolites formed by MFI nanosheets with different crystallite size (2-300 nm) which were obtained using gemini-surfactants with different alkyl chain lengths. FT-IR results, using pyridine (Py) and 2,6-di-tert-butylpyridine (DTBPy) as base probe molecules, as was introduced before to study the external (accessible) versus the internal (no accessible) acidities in delaminated zeolites, showed that the concentration of external acid sites increased with decreasing crystallite size.[98, 172] Although the external acid sites were weaker than the internal sites, they still catalyzed n-octane cracking process. It was notorious that the external acid sites of zeolites exhibited remarkably higher steam stability at high temperatures (873 K) than the internal acid sites, being this fact verified for the methanol to dimethylether (DME) and gasoline conversion, and the Claisen-Schmidt condensation when bulky substrates and intermediates are involved (Figure 26).[173] Additionally, the Brönsted acid sites on the external surfaces of MFI nanosheets were analyzed by the ^{31}P NMR chemical shifts of the adsorbed trimethylphosphine oxide and tributylphosphine oxide. The results revealed three types of Brönsted acid sites with different strengths on external surfaces, being four the types inside the internal micropores located into the zeolitic layers. Interestingly, a linear correlation was established between the number of external strongest acid sites and the catalytic activity in decalin cracking for different lamellar MFI zeolites.[174]
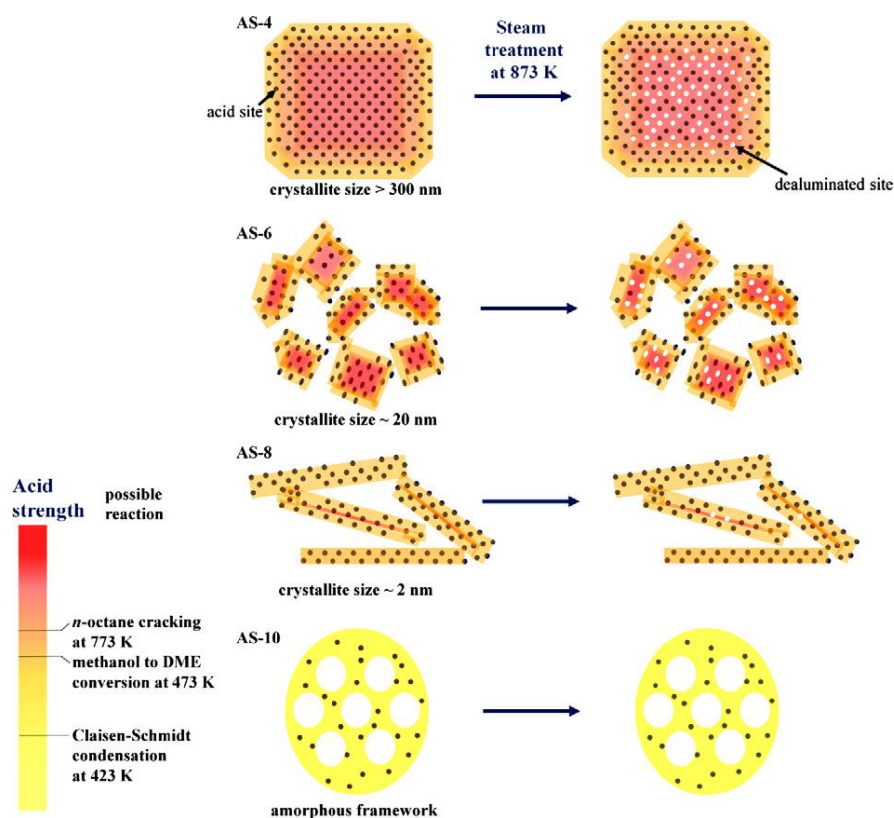
Figure 26. Schematic representation of the spatial distribution, strength, and steam stability of the acid sites in the lamellar MFI zeolites obtained using gemini-surfactants as surfactant directing agents (according to reference 173).

Nanosheets with an MFI zeolite topology exhibited a long catalytic lifetime and high selectivity for the production of ε-caprolactam through gas-phase Beckmann rearrangement of cyclohexanone oxime, being detectable a cooperative effect between surface Brönsted acid sites and silanol groups distributed along the MFI nanosheets.[175] Similar results for the Beckmann rearrangement of the bulkier cyclododecanone oxime were previously observed with the ITQ-2 delaminated zeolite.[133] The beneficial effect of large external surface was also observed for toluene disproportionation and its alkylation process.[176] Furthermore, the high accessibility of this type of multilamellar zeolites allowed the homogeneous deposition onto individual MFI zeolitic layers of isolated and stabilized Fe or Pt nanoparticles (NPs), minimizing the possible agglomeration phenomenon, as it was previously observed, and was described above, for the delaminated zeolites.[120] These bi-functional layered catalysts were successfully used for selective oxidation of benzene with nitrous oxide, n-decane isomerization and n-heptane hydroisomerization, showing these last results that the product selectivity to branched isomers was strongly improved by decreasing zeolite crystal thickness of MFI nanosheets. This selectivity improvement was due to the short diffusion way for branched products to get away before cracking process.[177, 178, 179] The results are perfectly in line with the previous hydroisomerization – hydrocracking results on bi-functional catalysts obtained with ITQ-2.[96]

It is important to point out that, following similar synthesis procedures, isomorphic titanosilicate MFI nanosheets of single-unit-cell thickness were also prepared with diquaternary ammonium surfactants as template molecules. The resultant titanium multi-lamellar MFI-type zeolites exhibited good catalytic activities and epoxide selectivity for bulky

substrates in olefins epoxidation reactions, using H_2O_2 or *tert*-butyl hydroperoxide as oxidant agents. Additionally, improved catalytic results were obtained by increasing surface hydrophobicity through post-synthetic fluoride treatment with NH_4F that partially removed surface silanol groups (Figure 27).[180]
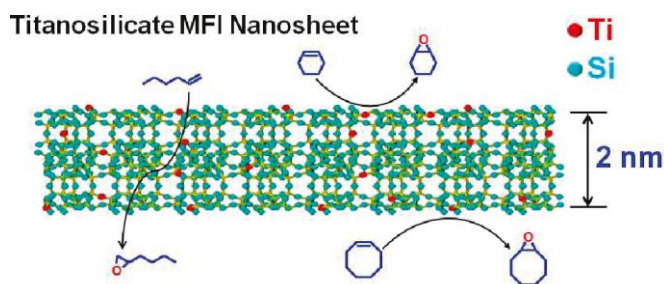

Figure 27. Schematic representation of titanium MFI-type nanosheet involved in 1-hexene, cyclohexene and cyclooctene epoxidation reactions (according to reference 180).

Although during the pseudomorphic crystallization of hierarchical micro/mesoporous BEA and MTW zeolites, in presence of cyclic diammonium molecules as structure directing agents (SDA), small crystallites formed by ordered zeolitic nanosheets were also detected,[181, 182] this innovative synthesis method for the synthesis of novel layered zeolitic materials practically have only been satisfactory when MFI-type nanosheets were finally crystallized. For this, important efforts were carried out to obtain other lamellar zeolites with different frameworks following this methodology, although only further advances have recently been achieved to prepare various phosphate materials, such as AlPOs, SAPOs, CoAPOs and GaPOs with AEL, ATO and AFI topologies.[183]

4- Synthesis of layered structures from germanosilicates

It was presented that the introduction of germanium in the synthesis of zeolites directs towards the formation of large and extra-large pore zeolites, containing double four (D4R) and double three (D3R) rings secondary building units.[184, 185, 186] Moreover, it was demonstrated that germanium very preferentially occupies D4R positions.[187, 188, 189, 190] One of these structures was ITQ-15,[191] which structure was shown to be formed by 14x12 ring pores and was denominated UTL, following the IZA code (see Figure 28a).[192, 193] Taking this account, Roth and Cejka *et al.* have recently prepared a novel type of layered zeolites, so-called ICP materials (IZA code PCR), formed by ferrieritic-type layers from the post-synthesis modification of large pore crystalline ITQ-15 germanosilicate (UTL structure). In fact, acid hydrolysis treatment of zeolite UTL resulted in the partial degradation of its structure with preservation of the initial dense layers previously connected by D4R germanium-rich bridges (Figure 28).[194, 195]
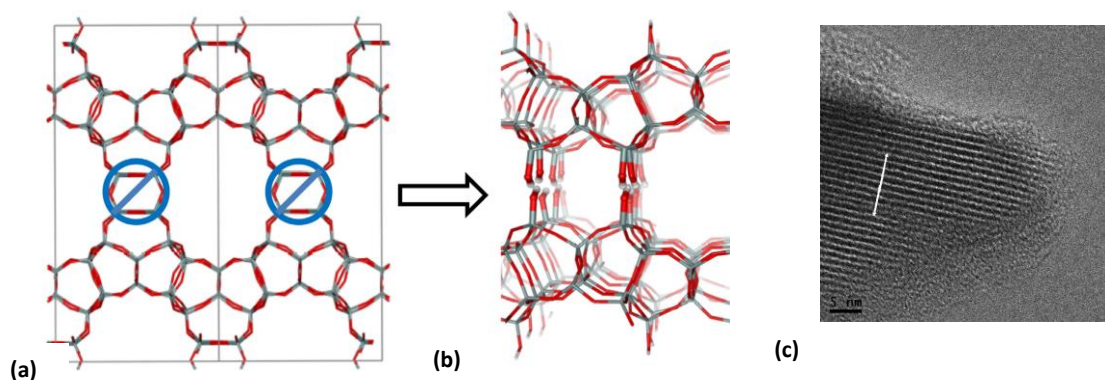
Figure 28. Preparation of layered zeolitic precursor IPC-1P (b) from 3D UTL structure (a) transformation upon removing the D4R units by acid hydrolysis process. In the scheme, the inter-layer interactions by hydrogen bonds between surface silanols are also shown (b). TEM image of the IPC-1P crystal in cross section (c), the white arrow representing 10 nm in length (according to reference 194 and 195).

The lamellar zeolite precursor ICP-1P obtained through this original 3D to 2D zeolite conversion was structurally modified through similar methodologies applied to another layered zeolitic precursors, such as MCM-22(P) or PREFER. Specifically, this layered precursor was swelled with CTMA molecules (ICP-1SW), pillared with interlayered silica units (ICP-1PI) and stabilized with intercalated silicon puncheons like expanded IEZ zeolites (ICP-2). It could also be re-converted to 3D zeolite with regular stacking of previously swollen ferrierite-like layers with octylamine (ICP-4), after calcination process, showing the versatility of this type of layered zeolitic precursors (Figure 29).[196, 197] On the contrary, direct calcination of layered precursor ICP-1P, without intercalated organic compounds, only led to a poorly ordered lamellar material (IPC-1).However, in the case of pillared solids, it was possible the formation of undesirable M41S mesoporous amorphous phases, cohabitating with layered ICP-type zeolites due to the strongly alkaline conditions used during the pillarization process in presence of surfactants as swelling agents.

It is remarkable that theoretical studies have also showed that this concept of inverse sigma transformation of a zeolite framework to generate new open structures by sheets' removal of intra-framework atoms could be extrapolated to other 3D zeolites.[198] It is the case of IM-12 zeolite (also UTL-type germanosilicate and isostructural to ITQ-15)[193] which is transformed in so-called COK-14 material through the dislodging germanate four-rings from acid leaching and successive annealing calcination treatment.[199] However, up to now, only successful results have been obtained with germanosilicates, involving the previous elimination of germanium-rich structural units. Moreover, the absence of active centers in the individual ferrieritic nanosheets of derived ICP materials, enormously limits the possible catalytic applications of these lamellar zeolites and further research efforts are necessary.[200]
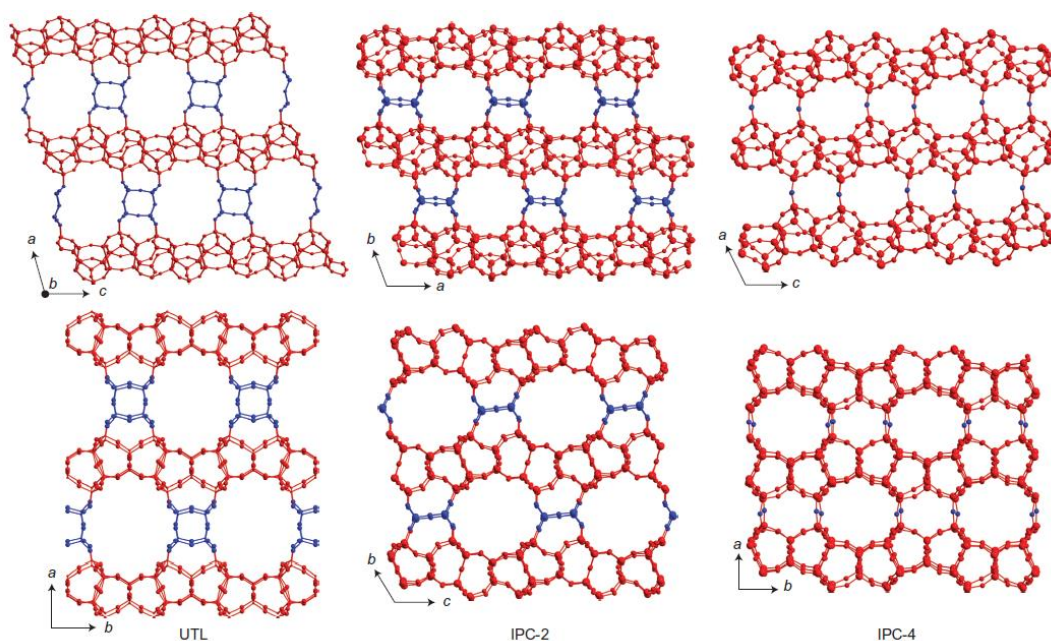
Figure 29. Structures of zeolites UTL, IPC-2 and IPC-4. In the scheme, it is shown the layer topology in all three materials (in red) together with the different sized linkers (blue) that lead to the different pore sizes in the materials (according to reference 197).

5- Other lamellar materials: Hybrid organic-inorganic layered aluminosilicates

Although with lower crystallinity, an elevated number of layered aluminosilicates have been described, showing similar versatility and physico-chemical properties than lamellar materials formed by individual zeolitic sheets, being the most studied kanemite, kenyaite and magadiite structures and their corresponding modified solids.[201] These families of layered aluminosilicates exhibit similar ability to be modified by swelling, intercalation or exfoliation that lamellar zeolites to generate expanded materials with high accessibility toward the active centers included into their framework.[202] Recently, taking advantage of these properties and together with the high variety of layered aluminosilicate precursors, several hybrid lamellar organic-inorganic materials have been prepared by the intercalation in the interlayer space of functional bridged silsesquioxanes, so-called disilanes, with general formula $_3$(R'O)Si-R-Si(OR')$_3$.[203] This methodology allowed the combination of the functions present both in the inorganic layers from the aluminosilicate precursors and those located in the organic pillars stabilized in the interlayer region from intercalated disilanes, extending largely the catalytic possibilities of these organic-inorganic layered solids to generate multi-functional catalysts.[204]

In this sense, Díaz *et al.* showed the possibility to prepare novel families of layered organic-inorganic hybrid materials synthesized by pillaring with disilanes containing amino, thiol, sulphonic, ethylene, viologen or nitroaniline compounds which were intercalated and stabilized between magadiite layers. Specifically, bridged silsesquioxanes reacted with the surface silanol groups of the inorganic layers of silicate, bonding covalently with them. It is important to remark that micro- and mesoporosity were also generated owing to the existence of porous galleries conformed by homogenously distributed organic linkers located in the interlayer space. These layered organic-inorganic hybrids exhibited a thermally stable network, and the organic spacers remained after elimination of the swelling agents by acid extraction.

The resultant materials were interesting not only as catalysts, but also as sensors and for nonlinear optics (Figure 30).[205, 206]
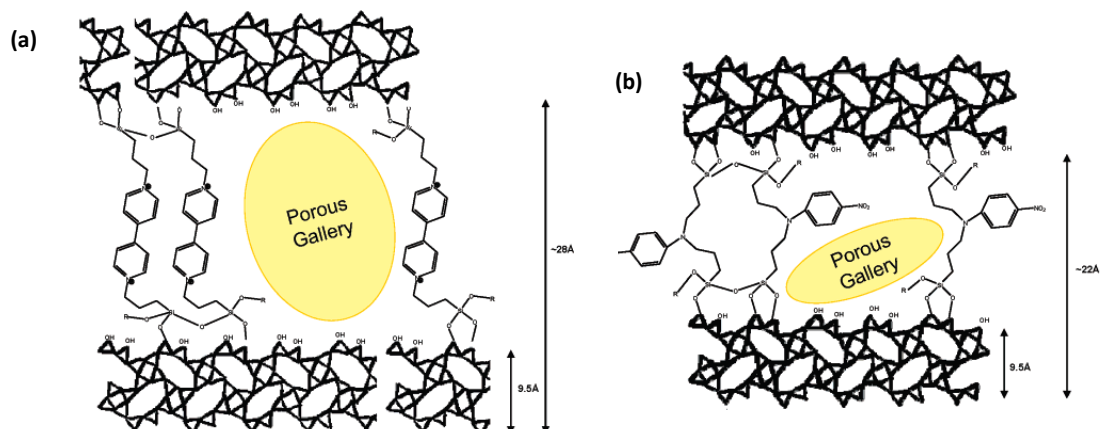

Figure 30. Schematic representation of layered hybrid organic-inorganic materials with (a) viologen and (b) nitroaniline units in the interlayer space (according to reference 205).

Despite the high potentiality of the lamellar hybrid materials prepared through the pillarization method using layered silicoaluminate precursors and bridged silsesquioxanes, several and, sometimes, complicated consecutive steps are required to obtain the final hybrid organic-inorganic materials. Normally, it is mandatory the synthesis, swelling and pillarization of staring layered silicoaluminate precursors, followed by the final extraction process. So, this type of methodology implies sophisticated and expensive synthesis routes. Furthermore, it has often been observed inhomogeneous distribution of organic pillars located in the interlayer space which may be a problem during the catalytic reactions due to diffusional associated problems, being interesting to improve this standard methodology to obtain more regular and stable lamellar organic-inorganic hybrid materials in only one step during the synthesis process.

6- Direct synthesis of layered hybrid organic-inorganic materials

Bellussi *et al.* have reported a new family of layered hybrid organic-inorganic materials, named as ECS (Eni Carbon Silicates), synthesized in only one step and using rigid arylic bridged silsesquioxanes, alkaline medium, sodium aluminate as additional sources (Si/Al ~1), hydrothermal conditions and in absence of structural directing agents.[207, 208] The result has been the generation of crystalline hybrid aluminosilicates with, in some cases, open porosity conformed by inorganic layers structured from $[AlO_4]$ and $[SiO_3C]$ tetrahedron which are separated by arylic bridges.[209] The crystal structure solution has shown that an elevated number of these lamellar materials contained a double microporous system: intra-layered conformed by porous channels, normally delimited by six member rings (6MR), and inter-layered due to the galleries generated between inorganic sheets and rigid aromatic linkers. These characteristics have allowed obtaining, in some cases, layered hybrid materials with specific surface areas and porous volumes close to 350 m^2g^{-1} and 0.8 cm^3g^{-1} (ECS-1). The open microporosity of the ECS materials is illustrated in Figure 31, taking ECS-3 material as example, being evidenced the regular and ordered arrangement between inorganic and organic sheets.[210, 211] Inside this family, it is remarkable the ECS-14 material that contained a system of

linear channels with 12-membered ring (12MR) openings, running along the [001] direction, resembling the pore architecture of the AFI framework type (Figure 32).[212]
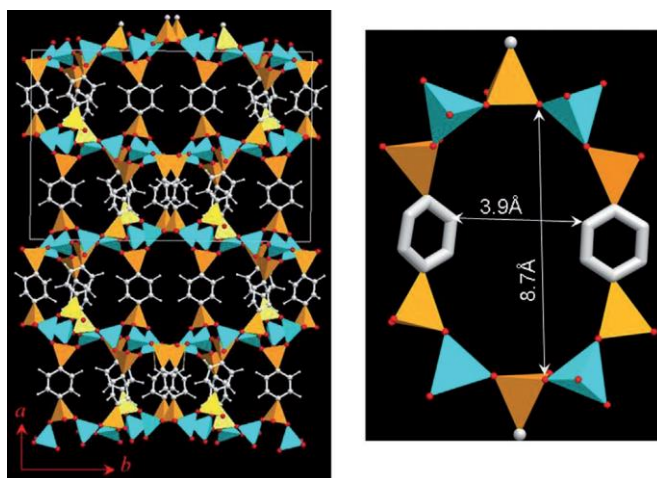

Figure 31. [001] projection of the ECS-3 framework structure (Al turquoise, Si yellow, C white, O red). Ellipsoidal ring of the interlayered sinusoidal channel along [001] direction is also illustrated (according to reference 210).
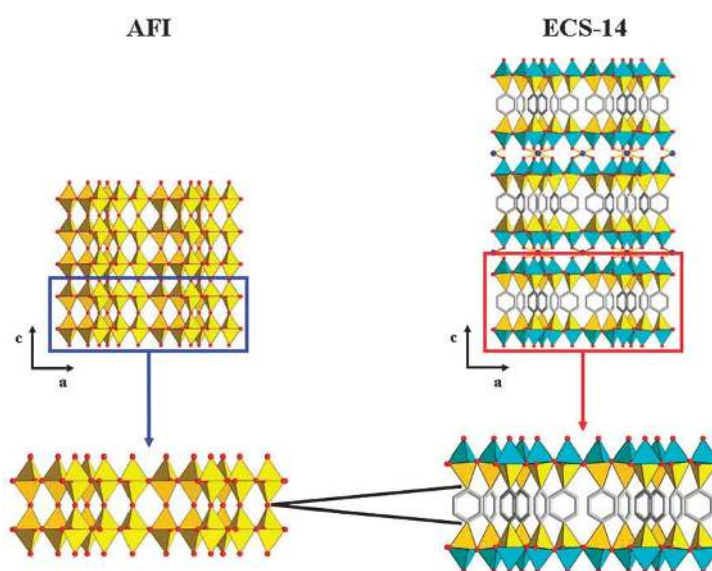
Figure 32. Scheme of the structures of SSZ-24 (AFI-type) and ECS-14, showing that the hybrid organic–inorganic layer is built through the insertion of phenylene rings between two layers of silica tetrahedral (according to reference 212).

Although highly elegant and interesting, these novel layered hybrid materials were only successfully prepared with rigid and non-active arylic fragments, this strongly restricting their catalytic possibilities. Moreover, the elevated concentration of intracrystalline sodium cations, the practically exclusive presence of framework aluminum in the inner and inaccessible part of the inorganic layers and the excessively reduced size of the microporous channels, delimited by 6MR, along the inorganic layers, make necessary further investigations to overcome these important limitations.

7- Outlook and future

The versatility of layered zeolitic materials to generate accessible and functional materials, particularly catalysts, has been analyzed along this perspective article-type. Specifically, it has been remarked the decisive role of lamellar precursors formed by ordered zeolitic sheets to obtain derived layered zeolites, through swelling, pillarization and/or exfoliation (delamination) post-synthesis treatments. The resultant materials exhibit high accessibility towards active sites, similar to standard mesoporous materials, but maintaining the characteristic stability and physico-chemical nature of zeolites. However, the reduced number of layered zeolitic precursors discovered so far (though the number is continuously increasing), can be a limitation to generate novel families of layered zeolites adapted to required necessities. For this, further efforts are necessary to generate new precursors through hydrothermal synthesis routes, using novel and specific pre-designed structural directing agents as templates of lamellar distributions, or favoring the structural disruption of pre-formed 3D zeolites to force the formation of zeolitic sheets. Alternatively, the combination of graphene assembled on zeolite surfaces to generate interesting novel lamellar composites may also be considered in the next future.[213]

On the other hand, the high catalytic activity of pillared or delaminated zeolites, particularly unique when bulk substrates, intermediates or products take part in the reaction process, could be even improved by the controlled incorporation of additional active centers during the structural modification of layered precursors. These further active sites (acid, base, redox, metallic nanoclusters or organometallic complexes) could be introduced, for instance, located along the pillars placed in the interlayer space or deposited onto the zeolitic layers, using the high surface area and the presence of high silanol groups' concentration onto the zeolitic sheets which would act as effective attaching covalent points. This approach would allow generating multi-functional catalysts, containing two or more active centers, isolated and separated at controlled molecular distances and avoiding their mutual neutralization, which could cooperatively act in the catalytic process. Remarkably, consecutive, multi-step or cascade reactions would be carried out with this type of multi-functional hybrid layered zeolites where only one recoverable solid catalyst would able to perform different catalytic steps, favoring more sustainable and economical processes based in the concept "*one catalyst for one-pot catalytic process*".[214]

References

1 T.E. Mallouk and J.A. Gavin, *Acc. Chem. Res*., 1998, **31**, 209-217.

2 H. Van Olphen, *An Introduction to Clay Colloid Chemistry*, John Wiley & Sons, New York, 1963.

3 K.S. Suslick and G.J. Price, *Annu. Rev. Mater. Sci*., 1999, **29**, 295-396.

4 (a) X. Du, D. Zhang, R. Gao, L. Huang, L. Shi and J. Zhang, *Chem. Commun*., 2013, **49**, 6770-6772; (b) H. Li, D. Zhang, P. Maitarad, L. Shi, R. Gao, J. Zhang and W. Cao, *Chem. Commun*., 2012, **48**, 10645-10647.

5 (a) H. Wang, D. Zhang, T. Yan, X. Wen, L. Shi and J. Zhang, *J. Mater. Chem*., 2012, **22**, 23745-23748; (b) D. Zhang, T. Yan, L. Shi, Z. Peng, X. Wen and J. Zhang, *J. Mater. Chem.,* 2012, **22**, 14696-14704.

6 T.J. Pinnavaia, *ACS Adv. Chem. Ser.,* 1995, **245**, 283-300.

7 R. Ravishankar, P.N. Joshi, S.S. Tamhankar, S. Sivasanker and V.P. Shiralkar, *Ads. Sci. Technol.*, 1998, **16**, 607-621.

8 Ch. Baerlocher, W.M. Meier and D.H. Olson, *Atlas of Zeolite Framework Types*, Elsevier, 2001; http://www.iza-structure.org/databases/

9 (a) W.J. Roth and D.L. Dorset, *Micropor. Mesopor. Mat*., 2011, **142**, 32-36; (b) W.J. Roth and J. Cejka, *Catal. Sci. Technol.,* 2011, **1**, 43-53.

10 M.E. Leonowicz, J.A. Lawton, S.L. Lawton and M.K. Rubin, *Science*, 1994, **264**, 1910-1913.

11 M.K. Rubin et al., *US Patent* 49454325, 1990.

12 L. Puppe and J. Weisser, *US Patent* 4439409, 1984.

13 (a) J.M. Bennett, C.D. Chang, S.L. Lawton, M.E. Leonowicz, D.N. Lissy and M.K. Rubin, *US Patent* 5236575, 1993; (b) S.L. Lawton et al., *J. Phys. Chem.*, 1996, **100**, 3788-3798.

14 (a) G.J. Kennedy, S.L. Lawton, A.S. Fung, M.K. Rubin and S. Stenernagel, *Catal. Today*, 1999, **49**, 385-399; (b) A.L.S. Santos-Marques, J.L.F. Monteiro and H.O. Pastore, *Micropor. Mesopor. Mat.*, 1999, **32**, 131-145; (c) D. Vuono, L. Pasqua, F. Testa, R. Aiello, A. Fonseca, T. Korany and J.B. Nagy, *Micropor. Mesopor. Mat*., 2006, **97**, 78-87.

15 A. Corma, C. Corell, J. Pérez-Pariente, J.M. Guil, R. Guil-López, S. Nicolopoulos, J. González-Calbet and M. Vallet-Regí, *Zeolites*, 1996, **16**, 7-14.

16 R. Ravishankar, T. Sen, V. Ramaswamy, H.S. Soni and S. Ganapathy, *Stud. Surf. Sci. Catal*., 1994, **84**, 331-338.

17 I. Guray, J. Warzywoda, N. Baç and A. Sacco, *Micropor. Mesopor. Mat.*, 1999, **15**, 241-251.

18 Y.M. Wang, X.T. Shu and M.Y. He, *Stud. Surf. Sci. Catal*., 2001, **135**, 194.

19 S.I. Zones, *European Patent* 231860, 1987.

20 I.Y. Chan, A.P. Labun, M. Pan and S.I. Zones, *Micropor. Mesopor. Mat.*, 1995, **3**, 409-418.

21 M.A. Camblor, A. Corma, M.J. Díaz-Cabañas and C. Baerlocher, *J. Phys. Chem. B*, 1998, **102**, 44-51.

22 J. Aguilar, A. Corma, F.V. Melo and E. Sastre, *Catal. Today*, 2000, **55**, 225-232.

23 M.A. Camblor, C. Corell, A. Corma, M.J. Díaz-Cabañas, S. Nicolopoulos, J.M. González-Calbet and M. Vallet-Regí, *Chem. Mater.*, 1996, **8**, 2415-2417.

24 M.A. Camblor, M.J. Díaz-Cabañas, C. Corell and A. Corma, *Spanish Patent* P9501553, 1995.

25 M.J. Díaz Cabañas, *Doctoral Thesis*, Instituto de Tecnología Química, Universidad Politécnica de Valencia, 1999.

26 S. Nicolopoulos, J.M. González-Calbet, M. Vallet-Regí, M.A. Camblor, C. Corell, A. Corma and M.J. Díaz-Cabañas, *J. Am. Chem. Soc.*, 1997, **119**, 11000-11005.

27 G. Bellusi, G. Perego, M.G. Cierici and A. Giusti, *European Patent* 293032, 1988.

28 R. Millini, G. Perego, W.O. Parker, G. Bellussi and L. Carluccio L., *Micropor. Mater.*, 1995, **4**, 221-230.

29 C.B. Khouw and M.E. Davis, *J. Catal.*, 1995, **151**, 77-86.

30 (a) T. Tatsumi, P. Wu, T. Komatsu and T. Yashima, *Chem. Lett.*, 2000, **7**, 774-775; (b) P. Wu, T. Tatsumi, T. Komatsu and T. Yashima, *J. Catal.*, 2001, **202**, 245-255; (c) P. Wu, T. Tatsumi, T. Komatsu and T. Yashima, *J. Phys. Chem. B,* 2001, **105**, 2897-2905; (d) P. Wu, Y. Liu, M. He and T. Tatsumi, *J. Catal.* 2004, **228**, 183-191; (e) P. Wu and T. Tatsumi*, Chem. Commun.,* 2001, **10**, 897-897; (f) M. Sasdharan, P. Wu and T. Tatsumi, *J. Catal.* 2002, **205**, 332-338; (g) P. Wu and T. Tatsumi, *J. Phys. Chem. B*, 2002, **106**, 748-753.

31 P. Wu and T. Tatsumi, *Chem. Commun.,* 2002, **10**, 1026-1027.

32 W. Fan, P. Wu, S. Namba and T. Tatsumi, *Angew. Chem. Int. Ed*., 2004, **43**, 236-240.

33 S.J. Kim, K.D. Jung and O.S. Joo, *J. Porous Mater.*, 2004, **11**, 211-218.

34 A.A. Teixeira-Neto, L. Marchese, G. Landi, L. Llai and H.O. Pastore*, Catal. Today*, 2008, **133-135**, 1-6.

35 Y. Wu, J. Wang, P. Liu, W. Zhang, J. Gu and X. Wang, *J. Am. Chem. Soc.,* 2010, **132**, 17989-17991.

36 T. Ikeda, Y. Akiyama, Y. Oumi, A. Kawai and F. Mizukami, *Angew. Chem. Int. Ed.*, 2004, **43**, 4892-4896.

37 D.L. Dorset and G.J. Kennedy, *J. Phys. Chem. B*, 2004, **108**, 15216-15222.

38 N. Tsunoji, T. Ikeda, Y. Ide, M. Sadakane and T. Sano, *J. Mater. Chem*., 2012, **22**, 13682-13690.

39 T. Ikeda, S. Kayamori, Y. Ouimi and F. Mizukami, *J. Phys. Chem. C*, 2010, **114**, 3466-3476.

40 H. Xu, B. Yang, J.G. Jiang, L. Jia, M. He and P. Wu, *Micropor. Mesopor. Mat*., 2013, **169**, 88-96.

41 L. Schereyeck, P. Caullet, J.C. Mougenel, J.L. Guth and B. Marler, *J. Chem. Soc*., *Chem. Commun*., 1995, **21**, 2187-2188.

42 L. Schereyeck, P. Caullet, J.C. Mougenel, J.L. Guth J.L. and B. Marler, *Microp. Mater.*, 1996, **6**, 259-271.

43 L. Schereyeck, P. Caullet, J.C. Mougenel, J.L. Guth and B. Marler, *Stud. Surf. Sci. Catal*., 1997, **105**, 1949-1956.

44 A. Corma, U. Díaz, M.E. Dómine and V. Fornés, *Angew. Chem. Int. Ed*., 2000, **39**, 1499-1501

45 T. Ikeda, S. Kayamori and F. Mizukami, *J. Mater. Chem*., 2009, **19**, 5518-5525.

46 B. Yang, J.G. Jiang, H. Xu, Y. Liu, H. Peng and P. Wu, *Appl. Catal. A- Gen.*, 2013, **455**, 107-113.

47 R.F. Lobo, A. Burton, R.J. Accardi, M. Falcioni and M.W. Deem, *Chem. Mater.*, 2000, **12**, 2936-2942.

48 R. Szostak, *US Patent* 4637923, 1987.

49 E.W. Valyocsik, *US Patent* 5068096, 1991.

50 R. Millini, L.C. Carluccio, A. Carati, G. Bellussi, C. Perego, G. Cruciani and S. Zanardi, *Micropor. Mesopor. Mater.,* 2004, **74**, 59-71.

51 A. Corma, U. Díaz and V. Fornés, *WO Patent* 02060815, 2002.

52 R. García, L. Gómez-Hortigüela, I. Díaz, E. Sastre and J. Pérez-Pariente, *Chem. Mater*., 2008, **20**, 1099-1107.

53 T.V. Whittam, *US Patent* 4397825, 1983.

54 S.J. Andrews, M.Z. Papiz, R. McMeeking, A.J. Blake, B.M. Lowe , K.R. Franklin, J.R. Helliwell and M.M. Harding, *Acta Crystallogr. Sect. B,* 1988, **44**, 73-77.

55 L.D. Rollmann, J.L. Schlenker, S.L. Lawton, C.L. Cannedy and G.J. Kennedy, *Micropor. Mesopor. Mat*., 2002, **53**, 179-193.

56 I.J.S. Lake and T.V. Whittam, *US Patent* 4400572, 1983.

57 S. Zanardi, A. Alberti, G. Cruciani, A. Corma, V. Fornés and M. Brunelli, *Angew. Chem. Int. Ed*., 2004, **43**, 4933-4937.

58 T. Araki, *Z. Kristallogr*., 1980, **152**, 207-213.

59 R.W. Hughes and M.T. Weller, *Micropor. Mesopor. Mat.*, 2002, **51**, 189-196.

60 B. Marler, M.A. Camblor and H. Gies, *Micropor. Mesopor. Mat.*, 2006, **90**, 87-101.

61 A.J. Blake, K.R. Franklin and B.M. Lowe, *J. Chem. Soc., Dalton Trans*., 1988, **10**, 2513-2517

62 G. Lagaly, *Solid State Ionics*, 1986, **22**, 43-51.

63 C.T. Kresge, *US Patent* 5229341, 1993**.**

64 C.T. Kresge, W.J. Roth, K.G. Simmons, J.C. Vartuli J.C., *WO Patent* 9211934, 1992**.**

65 W.J. Roth, C.T. Kresge, J.C. Vartuli, M.E. Leonowicz, A.S. Fung and S.B. McCullen S.B., *Stud. Surf. Sci. Catal.,* 1995, **94**, 301-308.

66 F. Eder, Y. He, G. Nivarthy and J.A. Lercher, *Recl. Trav. Chim. Pays-Bas*, 1996, **115**, 531-535.

67 Y.J. He, G.S. Nivarthy, F. Eder, K. Seshan and J.A. Lercher, *Micropor. Mesopor. Mat.*, 1998, **25**, 207-224.

68 A. Corma, V. Fornés, J. Martínez-Triguero, S.B.C. Pergher, *J. Catal.*, 1999, **186**, 57-63.

69 W.J. Roth, J.C. Vartuli and C.T. Kresge, *Stud. Surf. Sci. Catal.,* 2000, **129**, 501-508.

70 A. Chica, A. Corma, V. Fornés and U. Díaz, *WO Patent 0024673*, 2000.

71 W.J. Roth and C.T. Kresge, *Micropor. Mesopor. Mater*., 2011, **144**, 158-161.

72 J.O. Barth, J. Kornatowski and J.A. Lercher, *J. Mater. Chem.,* 2004, **12**, 369-373.

73 (a) J.O. Barth, A. Jentys, E.F. Iliopoulou, I.A. Vasalos and J.A. Lercher, *J. Catal.,* 2004, **227**, 117-129; (b) J. Kornatowski, J.O. Barth and J.A. Lercher, *Stud. Surf. Sci. Catal.,* 2005, **156**, 349-356.

74 (a) J.O. Barth, A. Jenyts, J. Kornatowski and J.A. Lercher, *Chem. Mater*., 2004, **16**, 724-730; (b) R. Schenkel, J.O. Barth, J. Kornatowski, A. Jenyts and J.A. Lercher, *Stud. Surf. Sci. Catal*., 2004, **154B***,* 1598-1605; (c) J.O. Barth, R. Schenkel, J. Kornatowski and J.A. Lercher, *Stud. Surf. Sci. Catal.,* 2001, **135**, 1525-1533.

75 S. Maheshwari, E. Jordan, S. Kumar, F.S. Bates, R.L. Penn, D.F. Shantz and M. Tsapatsis M., *J. Am. Chem. Soc*., 2008, **130**, 1507-1516.

76 D.X. Liu, A. Bhan, M. Tsapatsis and S. Al Hashimi, *ACS Catal*., 2011, **1**, 7-17.

77 A. Corma, *Chem. Rev*., 1995, **95**, 559-614.

78 P. Wu, Q. Kan, D. Wang, H. Xing, M. Jia and T. Wu, *Catal. Commun*., 2005, **6**, 449-454.

79 (a) M. Lallemand, O.A. Rusu, E. Dumitriu, A. Finiels, F. Fajula and V. Hulea, *Appl. Catal. A-Gen.*, 2008, **338**, 37-43; (b) M. Lallemand, O.A. Rusu, E. Dumitriu, A. Finiels, F. Fajula and V. Hulea, *Stud. Surf. Sci. Catal.,* 2008, **174B**, 1139-1142.

80 J. Aguilar, S.B.C. Pergher, C. Detoni, A. Corma, F.V. Melo and E. Sastre, *Catal. Today*, 2008, **133-135**, 667-672.

81 Y. Zhang, H. Xing, P. Yang, P. Wu, M. Jia, J. Sun and T. Wu, *React. Kinet. Catal. Lett.*, 2007, **90**, 45-52.

82 D. Meloni, E. Dumitriu, R. Monaci and V. Solinas*, Stud. Surf. Sci. Catal.,* 2008, **174B**, 1111-1114.

83 E. Dumitriu, I. Fechete, P. Caullet, H. Kessler, V. Hulea, C. Chelaru, T. Hulea and X. Bourdon, *Stud. Surf. Sci. Catal*., 2002, **142A**, 951-958.

84 A. Lacarrie, F. Luck, D. Swierczynski, F. Fajula and V. Hulea, *Appl. Catal. A-Gen.*, 2011, **402**, 208-217.

85 J. Barth, A. Jenyts and J.A Lercher, *Stud. Surf. Sci. Catal*., 2004, **154C**, 2441-2448.

86 (a) J. Ding, H. Liu, P. Yuan, G. Shi and X. Bao, *ChemCatChem*, 2013, **5**, 2258-2269; (b) J. Zhu, Y. Cui, Y. Wang and F. Wei, *Chem. Commun*., 2009, **22**, 3282-3284; (c) Y.J. Wang, Y. Tang, X.D. Wang, A.G. Dong, W. Shan and Z. Gao, *Chem. Lett*., 2001, **11**, 1118-1119; (d) K.H. Rhodes, S.A. Davis, F. Caruso, B. Zhang and S. Mann, *Chem. Mater*., 2000, **12**, 2832-2834.

87 A. Corma, U. Díaz, T. García, G. Sastre and A. Velty, *J. Am. Chem. Soc*., 2010, **132**, 15011-15021.

88 S. Inagaki and T. Tatsumi, *Chem. Commun*., 2009, **18**, 2583-2585.

89 P. Wu, J. Ruan, L. Wang, L. Wu, Y. Wang, Y. Liu, W. Fan, M. He, O. Terasaki and T. Tatsumi, *J. Am. Chem. Soc*., 2008, **130**, 8178-8187.

90 L. Wang, Y. Wang, Y. Liu, H. Wu, X. Li, M. He and P. Wu, *J. Mater. Chem*., 2009, **19**, 8594-8602.

91 W. Fan, P. Wu, S. Namba and T. Tatsumi, *Angew. Chem. Int. Ed*., 2004, **43**, 236-240.

92 J. Ruan, P. Wu, B. Slater and O. Terasaki, *Angew. Chem. Int. Ed.,* 2005, **44**, 6719-6723.

93 (a) T. Tatsumi, W. Peng and T. Katsuyuki, *US Patent* 7326401B2, 2008; (b) M. Moliner and A. Corma, *Chem. Mater*., 2012, **24**, 4371-4375.

94 S.B.C. Pergher, *Doctoral Thesis*, Instituto de Tecnología Química, Universidad Politécnica de Valencia, 1997.

95 A. Corma, V. Fornés and S.B.C. Pergher, *WO Patent* 9717290A1, 1997.

96 A. Corma, V. Fornés , S.B.C. Pergher, Th.L. Maesen and J.G. Buglass, *Nature*, **1998**, *396*, 353-356.

97 A. Corma,V. Fornés, J.M. Guil, S.B.C. Pergher, Th.L. Maesen and J.G. Buglass*, Micropor. Mesopor. Mater.*, 2000, **38**, 301-309.

98 A. Corma, U. Díaz, V. Fornés, J.M. Guil, J. Martínez-Triguero and E.J. Creyghton, *J. Catal.*, 2000, **191**, 218-224.

99 G. Sastre, R. Catlow, A. Chica and A. Corma, *J. Phys. Chem. B*, 2000, **104**, 416-422.

100 I. Ogino, M.M. Nigra, S.J. Hwang, J.M. Ha, T. Rea, S.I. Zones and A. Katz, *J. Am. Chem. Soc*., 2011**, 133**, 3288-3291.

101 P. Wu, D. Nuntasri, J. Ruan, Y. Liu, M. He, W. Fan, O. Terasaki and T. Tatsumi, *J. Phys. Chem. B*, 2004, **108**, 19126-19131.

102 A. Corma, U. Diaz, V. Fornés, J.L. Jordá, M.E. Dómine and F. Rey, *Chem. Commun.* 1999, **9**, 779-780.

103 W. Adam, A. Corma, H. García and O. Weichold, *J. Catal.*, 2000, **196**, 339-344.

104 (a) P. Serna, L.A. Baumes, M. Moliner and A. Corma, *J. Catal.*, 2008, **258**, 25-34; (b) L.A. Baumes, P. Serna and A. Corma, *Appl. Catal. A-Gen.*, 2010, **381**, 197-208.

105 H. Masahiro, S. Keisuke and A. Corma, *US Patent* 20100069677, 2010.

106 A.S. Fung, S.L. Lawton and W.J. Roth, *US Patent* 5362697, 1994.

107 (a) R.F.Lobo and G.J. Gopalakrishan, *Micropor. Mesopor. Mater.*, 2000, **40**, 9-23; (b) P.P. Yang, J.F. Yu, Z.L. Wang, M.P. Xu, Q.S. Liu, X.W. Yang and T.H. Wu, *Cat. Commun*., 2005, **6**, 107-111.

108 A. Corma, M.J. Díaz-Cabañas, M. Moliner and C. Martínez, *J. Catal.*, 2006, **241**, 312-318.

109 W.J. Roth, D.L. Dorset and G.J. Kennedy, *Micropor. Mesopor. Mater*., 2011, **142**, 168-177.

110 J. Wang, X. Tu, W. Hua, Y. Yue and Z. Gao, *Micropor. Mesopor. Mater.,* 2011, **142**, 82-90.

111 H.J. Jung, S.S. Park, C.H. Shin, Y.K. Park and S.B. Hong, *J. Catal.*, 2006, **245**, 65-74.

112 S. Inagaki, K. Kamino, E. Kikuchi and M. Matsukata, *Appl. Catal. A-Gen.*, 2007, **318**, 22-27.

113 A. Corma and H. García, *Catal. Today*, 1997, **38**, 257-308.

114 P. Botella, A. Corma, R.H. Carr and C.J. Mitchell, *Appl. Catal. A-Gen.*, 2011, **398**, 143-149.

115 A. Corma, P. Botella and C. Mitchell, *Chem. Commun*., 2004, **17**, 2008-2010.

116 P. Botella, J.K.P. Bosman, A. Corma and C.J. Mitchell, *US Patent* 7238840, 2007.

117 H.K. Min, M.B. Park and S.B. Hong, *J. Catal*., 2010, **271**, 186-194.

118 J. Wang, F. Zhang, W. Hua, Y. Yue and Z. Gao, *Catal. Commun*., 2012, **18**, 63-67.

119 A. Corma, V. González-Alfaro and A.V. Orchillés, *J. Catal.,* 2001, **200**, 34-44.

120 A. Corma, A. Martínez, V. Martínez-Soria, *J. Catal*., 2001, **200**, 259-269.

121 G. Prieto, A. Martínez, P. Concepción and R. Moreno-Tost, *J. Catal*., 2009, **266**, 129-144.

122 A. Martínez and G. Prieto, *J. Catal.,* 2007, **245**, 470-476.

123 P. Concepción, C. López, A. Martínez and V.F. Puntes, *J. Catal.*, 2004, **228**, 321-332.

124 A. Martínez, S. Valencia, R. Murciano, H.S. Cerqueira, A.F. Costa and E.F. S.-Aguiar, *Appl. Catal. A-Gen.,* 2008, **346**, 117-125.

125 A. Martínez, E. Peris and G. Sastre, *Catal. Today*, 2005, **107-108**, 676-684.

126 A. Chica and S. Sayas, *Catal. Today*, 2009, **146**, 37-43.

127 M.J. Climent, A. Corma, V. Fornés, H. García, S. Iborra, J. Miralles and I. Rodríguez, *Stud. Surf. Sci. Catal.,* 2001, **135**, 3719-3726.

128 I. Rodríguez, M.J. Climent, S. Iborra, V. Fornés and A. Corma, *J. Catal*., 2000, **192**, 441-447.

129 C.C. Aquino, H.O. Pastore, A.F. Masters and T. Maschmeyer, *ChemCatChem*, 2011, **3**, 1759-1762.

130 M.J. Climent, A. Corma and A. Velty, *Stud. Surf. Sci. Catal.,* 2001, **135**, 3727-3735.

131 M.J. Climent, A. Corma and A. Velty*, Appl. Catal. A-Gen.*, 2004, **263**, 155-161.

132 M.J. Climent, A. Corma and S. Iborra, *J. Catal.*, 2005, **233**, 308-316.

133 P. Botella, A. Corma, S. Iborra, R. Montón, I. Rodríguez and V. Costa, *J. Catal.*, 2007, **250**, 161-170.

134 M.V. Gómez, A. Cantín, A. Corma A. and A. De la Hoz, *J. Mol. Catal. A-Chem.*, 2005, **240**, 16-21.

135 J. Wang, S. Jaenicke , G.K. Chuah, W. Hua, Y. Yue and Z. Gao, *Catal. Commun.*, 2011, **12**, 1131-1135.

136 M.M. Antunes, S. Lima, A. Fernandes, M. Pillinger, M.F. Ribeiro and A.A. Valente, *Appl. Catal. A-Gen.*, 2012, **417-418**, 243-252.

137 A. Fuerte, A. Corma, M. Iglesias, E. Morales and F. Sánchez, *J. Mol. Catal. A-Chem.,* 2006, **246**, 109-117.

138 C. Baleizao, B. Gigante, M.J. Sabater, H. García and A. Corma, *Appl. Catal. A-Gen.*, 2002, 228, 279-288.

139 V. Ayala, A. Corma, M. Iglesias, J.A. Rincón J.A. and F. Sánchez, *J. Catal.*, 2004, **224**, 170-177.

140 C. González-Arellano, A. Corma, M. Iglesias and F. Sánchez, *Adv. Synth. Catal*., 2004, **346**, 1316-1328.

141 C. González-Arellano, A. Corma, M. Iglesias and F. Sánchez, *Adv. Synth. Catal.,* 2004, **346**, 1758-1764.

142 I. Domínguez, V. Fornés and M.J. Sabater, *J. Catal.*, 2004, **228**, 92-99.

143 C. Baleizao, G. Barbara, H. García and A. Corma*, J. Catal.*, 2003, **215**, 199-207.

144 A. Fuerte, A. Corma and F. Sánchez, *Catal. Today*, 2005, **107-108**, 404-409.

145 A. Corma, E. Gutiérrez-Puebla, M. Iglesias, A. Monge, S. Pérez-Ferreras and F. Sanchez, *Adv. Synth. Catal.,* 2006, **348**, 1899-1907.

146 A. Corma, C. González-Arellano, M. Iglesias, S. Pérez-Ferreras and F. Sánchez, *Synlett*, 2007, **11**, 1771-1774.

147 A. Macario, A. Katovic, G. Giordano, L. Forni, F. Carloni, A. Filippini and L. Setti, *Stud. Surf. Sci. Catal.,* 2005, **155**, 381-394.

148 A. Corma, V. Fornés, M.S. Galletero, H. García and C.J. Gómez-García, *Phys. Chem. Chem. Phys*., 2001, **3**, 1218-1222.

149 M.S. Galletero, A. Corma, B. Ferrer, V. Fornés and H. García, *J. Phys. Chem. B*, 2003, **107**, 1135-1141.

150 A. Corma, V. Fornés, M.S. Galletero, H. García and J.C. Scaiano, *Chem. Commun*., 2002, 4, 334-335.

151 A. Corma, U. Díaz, B. Ferrer, V. Fornés, M.S. Galletero and H. García, *Chem. Mater*., 2004, **16**, 1170-1176.

152 P. Atienzar, A. Corma, H. García and J.C. Scaiano, *Chem. Mater*., 2004, **16**, 982-987.

153 A. Corma, M.S. Galletero, H. García, E. Palomares and F. Rey, *Chem. Commun*., 2002, **10**, 1100-1101.

154 H. Dathe, C. Sedlmair, A. Jentys, J.A. Lercher, *Stud. Surf. Sci. Catal*., 2004, **154C**, 3003-3009.

155 S.T. Yang, J.Y. Kim, J. Kim and W.S. Ahn, *Fuel*, 2012, **97**, 435-442.

156 (a) J. Pawlesa, A. Zukal and J. Cejka, *Adsorption*, 2007, **13**, 257-265; (b) I. Domínguez, J. Pawlesa, A. Zukal and J. Cejka, *Stud. Surf. Sci. Catal.*, 2008, **174**, 603-606; (c) A. Zukal, J. Pawlesa and J. Cejka, *Adsorption*, 2009, **15**, 264-270; (d) A. Zukal, I. Domínguez, J. Mayerova and J. Cejka, *Langmuir*, 2009, **25**, 10314-10321.

157 A. Corma, A. Chica, U. Díaz and V. Fornés, *WO Patent* 0007722, 2000.

158 (a) A. Corma , V. Fornés and U. Díaz, *WO Patent* 0105705, 2001; (b) A. Corma, V. Fornés and U. Díaz, *Chem. Commun*., **2001**, *24*, 2642-2643.

159 A. Corma, U. Díaz and V. Fornés, *WO Patent* 02060816, 2002.

160 A. Corma, U. Díaz, M.E. Dómine and V. Fornés, *J. Am. Chem. Soc*., 2000, **122**, 2804-2809.

161 A. Corma, U. Díaz, M.E. Dómine and V. Fornés, *Chem. Commun*., 2000, **2**, 137-138.

162 A. Corma, V. Fornés, J.L. Jordá, F. Rey, R. Fernández-Lafuente, J.M. Guisan and C. Mateo, *Chem. Commun.,* 2001, **5**, 419-420.

163 A. Corma, V. Fornés and F. Rey, *Adv. Mater*., 2002, **14**, 71-74.

164 E. Dumitriu, F. Secundo, J. Patarin and I. Fechete, *J. Mol. Catal. B-Enzym*., 2003, **22**, 119-133.

165 B. Solsona, J.M. López-Nieto and U. Díaz, *Micropor. Mesopor. Mater*., 2006, **94**, 339-347.

166 E.A. Eilertsen, I. Ogino, S.J. Hwang, T. Rea, S. Yeh, S.I. Zones and A. Katz, *Chem. Mater*., 2011, **23**, 5404-5408.

167 M. Choi, K. Na, J. Kim, Y. Sakamoto, O. Terasaki and R. Ryoo, *Nature*, 2009, **461**, 246-249.

168 W. Park, D. Yu, K. Na, K.E. Jelfs, B. Slater, Y. Sakamoto and R. Ryoo, *Chem. Mater*., 2011, **23**, 5131-5137.

169 J. Jung , C. Jo, K. Cho and R. Ryoo, *J. Mater. Chem*., 2012, **22**, 4637-4640.

170 K. Na, M. Choi, W. Park, Y. Sakamoto, O. Terasaki and R. Ryoo*, J. Am. Chem. Soc.,* 2010, **132**, 4169-4177.

171 K. Na, W. Park, Y. Seo and R. Ryoo, *Chem. Mater*., 2011, **23**, 1273-1279.

172 A. Corma, V. Fornés, L. Forni, F. Márquez, J. Martínez-Triguero and D. Moscotti, *J. Catal.,* 1998, **179**, 451-458.

173 K. Kim, R. Ryoo, H.D. Jang and M. Choi, *J. Catal*., 2012, **288**, 115-123.

174 Y. Seo, K. Cho, Y. Jung and R. Ryoo R., *ACS Catal*., 2013, **3**, 713-720.

175 J. Kim, W. Park and R. Ryoo, *ACS Catal*., 2011, **1**, 337-341.

176 C. Jo, R. Ryoo, N. Zilkova, D. Vitvarova and J. Cejka, *Catal. Sci. Technol*., 2013, **3**, 2119-2129.

177 A.J.J. Koekkoek, W. Kim, V. Degirmenci, H. Xin, R. Ryoo and E.J.M. Hensen, *J. Catal*., 2013, **299**, 81-89.

178 E. Verheyen, C. Jo, M. Kurttepeli, G. Vanbutsele, E. Gobechiya, T.I. Koranyi, S. Bals, G. Van Tendeloo, R. Ryoo, C.E.A. Kirschhock and J.A. Martens, *J. Catal*., 2013, **300**, 70-80.

179 J. Kim, W. Kim, Y. Seo, J.C. Kim and R. Ryoo, *J. Catal*., 2013, **301**, 187-197.

180 K. Na, C. Jo, J. Kim, W.S. Ahn and R. Ryoo, *ACS Catal*., 2011, **1**, 901-907.

181 M. Choi, K. Na and R. Ryoo, *Chem. Commun*., 2009, **20**, 2845-2847.

182 K. Na, M. Choi and R. Ryoo, *J. Mater. Chem*., 2009, **19**, 6713-6719.

183 Y. Seo, S. Lee, C. Jo and R. Ryoo, *J. Am. Chem. Soc*., 2013, **135**, 8806-8809.

184 A. Corma, M.T. Navarro, F. Rey, J. Rius and S. Valencia, *Angew. Chem. Int. Ed*., 2001, **40**, 2277-2280.

185 A. Corma, M.J. Díaz-Cabañas, J. Martínez-Triguero, F. Rey and J. Rius, *Nature*, 2002, **418**, 514-517.

186 A. Corma, M.J. Díaz-Cabañas, J. Jiang, M. Afeworki, D.L. Dorset, S.L. Soled and K.G. Strohmaierb, *PNAS*, 2010, **107**, 13997-14002.

187 A. Corma, F. Rey, S. Valencia, J.L. Jordá and J. Rius, *Nat. Mater.*, 2003, **2**, 493-497.

188 R. Castañeda, A. Corma, V. Fornés, F. Rey and J. Rius, *J. Am. Chem. Soc.*, 2003, **125**, 7820-7821.

189 A. Corma, M.T. Navarro, F. Rey and S. Valencia, *Chem. Commun.*, 2001, **16**, 1486-1487.

190 A. Corma, M.J. Díaz-Cabañas and F. Rey, *Chem. Commun.*, 2003, **9**, 1050-1051.

191 A. Corma, M.J. Díaz-Cabañas and F. Rey, *WO Patent*, 0203820, 2002.

192 A. Corma, M.J. Díaz-Cabañas, F. Rey, S. Nicolopoulus and K. Boulahya, *Chem. Commun.*, 2004, **12**, 1356-1357.

193 J.L. Paillaud, B. Harbuzaru, J. Patarin and N. Bats, *Science*, 2004, **304**, 990-992.

194 W.J. Roth, O.V. Shvets, M. Shamzhy, P. Chlubna, M. Kubu, P. Nachtigall and J. Cejka, *J. Am. Chem. Soc.,* 2011, **133**, 6130-6133.

195 O.V. Shvets, P. Nachtigall, W.J. Roth and J. Cejka, *Micropor. Mesopor. Mater.*, 2013, **182**, 229-238.

196 P. Chlubna, W.J. Roth, H.F. Greer, W. Zhou, O. Shvets, A. Zukal, J. Cejka and R.E. Morris, *Chem. Mater.*, 2013, **25**, 542-547.

197 W.J. Roth, P. Nachtigall, R.E. Morris, P.S. Wheatley, V.R. Seymour, S.E. Ashbrook, P. Chlubna, L. Grajciar, M. Polozij, A. Zukal, O. Shvets and J. Cejka, *Nature Chem.*, 2013, **5**, 628-633.

198 L. Grajciar, O. Bludsky, W.J. Roth and P. Nachtigall, *Catal. Today*, 2013, **204**, 15-21.

199 E. Verheyen, L. Joos, K. Van Havenbergh, E. Breynaert, N. Kasian, E. Gobechiya, K. Houthoofd, C. Martineau, M. Hinterstein, F. Taulelle, V. Van Speybroeck, M. Waroquier, S. Bals, G. Van Tendeloo, C.E.A. Kirschhock and J.A. Martens, *Nature Mater.*, 2012, **11**, 1059-1064.

200 N. Kasian, E. Verheyen, G. Vanbutsele, K. Houthoofd, T.I. Koranyi, J.A. Martens and C.E.A. Kirschhock, *Microp. Mesop. Mater.*, 2013, **166**, 153-160.

201 G.G. Almond, R.K. Harris and K.R. Franklin, *J. Mater. Chem.,* 1997, **7**, 681-687.

202 J.S. Dailey and T.J. Pinnavaia, *Chem. Mater.* 1992, **4**, 855-863.

203 K.J. Shea, D.A. Loy and O. Webster, *J. Am. Chem. Soc.*, 1992, **114**, 6700-6710.

204 U. Díaz, D. Brunel and A. Corma, *Chem. Soc. Rev.*, 2013, **42**, 4083-4097.

205 U. Díaz, A. Cantín and A. Corma, *Chem. Mater.*, 2007, **19**, 3686-3693.

206 U. Díaz, A. Cantín, T. García and A. Corma, *Stud. Surf. Sci. Catal.*, 2008, **174A**, 337-340.

207 G. Bellussi, A. Carati, E. Di Paola, R. Millini, W.O.N. Parker Jr, C. Rizzo and S. Zanardi, *Microp. Mesop. Mater.,* 2008, **113**, 252.

208 G. Bellussi, A. Carati, C. Rizzo, U. Díaz Morales, S. Zanardi, W.O.N. Parker and R. Millini, *WO Patent* 017513, 2008.

209 S. Zanardi, G. Bellussi, A. Carati, E. Di Paola, R. Millini, W.O.N. Parker and C. Rizzo, *Stud. Surf. Sci. Catal.*, 2008, **174B**, 965-968.

210 G. Bellussi, E. Montanari, E. Di Paola, R. Millini, A. Carati, C. Rizzo, W.O.N. Parker Jr, M. Gemmi, E. Mugnaioli and S. Zanardi, *Angew. Chem. Int. Ed.*, 2012, **51**, 666-669.

211 S. Zanardi, W.O. Parker, A. Carati, G. Botti and E. Montanari, *Micropor. Mesopor. Mater*., 2013, **172**, 200-205.

212 G. Bellussi, R. Millini, E. Montanari, A. Carati, C. Rizzo, W.O.N. Parker, G. Cruciani, A. De Angelis, L. Bonoldi and S. Zanardi, *Chem. Commun*., 2012, **48**, 7356-7358.

213 (a) M. Zhang, B. Gao, K. Pu, Y. Yao and M. Inyang, *Chem. Eng. J*., 2013, **223**, 556-562; (b) Y. Matsuo, S. Ueda, K. Konishi, J.P. Marco-Lozar, D. Lozano-Castello and D. Cazorla-Amoros, *Int. J. Hydrogen Energ*., 2012, **37**, 10702-10708; (c) H. Nishihara, H. Itoi, T. Kogure, P.X. Hou, H. Touhara, F. Okino and T. Kyotani, *Chem. Eur. J.,* 2009, **15**, 5355-5363.

214 M. J. Climent, A. Corma and S. Iborra, *ChemSusChem*, 2009, **2**, 500–506.